https://rbgeomorfologia.org.br/
ISSN 2236-5664

Revista Brasileira de Geomorfologia

v. 25, nº 1 (2024)

http://dx.doi.org/10.20502/rbg.v25i1.2467

Research Article

Interactions between Cenozoic tectonics and landscape dynamics in Londrina, Paraná, Brazil

Interações entre tectônica Cenozoica e dinâmica da paisagem em Londrina, Paraná, Brazil

Ana Cecília Branco Sowinski [1], Eduardo Salamuni [2], Marcilene dos Santos [3] e Salomão Silva Calegari [4]

[1] UFPR - Federal University of Paraná, Department of Geology, Curitiba-PR, Brazil. acbsowinski@gmail.com
ORCID: https://orcid.org/0009-0000-7232-9153
[2] UFPR - Federal University of Paraná, Department of Geology, Curitiba-PR, Brazil, salamuni@ufpr.br
ORCID: https://orcid.org/0000-0001-5179-0450
[3] UNESP - São Paulo State University, School of Sciences, Technology and Education, Department of Geography and Planning, Campus Ourinhos, Ourinhos -SP, Brazil, marcilene.santos@unesp.br
ORCID: https://orcid.org/0000-0002-4883-1511
[4] UFES - Federal University of Espírito Santo, Department of Geology, Alegre-ES, Brazil, salomaocalegari@ufes.br
ORCID: https://orcid.org/0000-0002-9059-0432

Recebido: 18/08/2023; Aceito: 24/01/2024; Publicado: 27/03/2024

Abstract: The Londrina City, located in southern Brazil, is situated on the basalt of the Paraná Igneous Province (PIP), near tectonic structures such as the Guaxupé faults and the São Jerônimo-Curiúva and São Sebastião lineaments, with a history of reactivation in the Cenozoic. Between 2015 and 2018, low-magnitude earthquakes hit the municipality, suggesting a possible connection with these structures. This study investigates the relationship between Cenozoic tectonics and geomorphological dynamics, combining quantitative geomorphological analysis with field analysis of faults. The results reveal signs of tectonic control on the landscape, with two pulses of regional uplift/base level drop affecting the drainage network. Reactivated segments, especially at intersections of NE and NW structures, influence dynamics, with variations in uplift rates between basins and block rotation under a transtensive regime. Recent earthquakes are related to the reactivation of an N50-60E fault scarp, possibly the Guaxupé Fault, indicating recurrent tectonic movement. Paleostress analyses identify three deformation pulses, highlighting the complexity of landscape evolution in intraplate regions. These findings enhance understanding of regional tectonics, emphasizing the need to comprehend landscape evolution in interior plate areas, such as the South American Plate.

Keywords: Tectonic Geomorphology; Landscape Evolution; Geomorphic Indices; Brittle Tectonics.

Resumo: Localizada no sul do Brasil, Londrina está situada sobre os basaltos da Província Ígnea do Paraná (PIP), próxima a estruturas tectônicas como as falhas de Guaxupé e os lineamentos São Jerônimo-Curiúva e São Sebastião, com histórico de reativação no Cenozoico. Entre 2015 e 2018, sismos de baixa magnitude atingiram o município, sugerindo uma possível relação com essas estruturas. Este estudo investiga a relação entre a tectônica cenozoica e a dinâmica geomorfológica, combinando análise geomorfológica quantitativa com análise de falhas em campo. Os resultados revelam sinais de controle tectônico na paisagem, com dois pulsos de soerguimento/queda de nível de base regionais afetando a rede de drenagem. Segmentos reativados, especialmente em interseções de estruturas NE e NW, influenciam a dinâmica, com variações nas taxas de soerguimento entre bacias e rotação de blocos sob regime transtensivo. Sismos recentes estão relacionados à reativação de uma escarpa de falha N50-60E, possivelmente a Falha de Guaxupé, indicando movimentação tectônica recorrente. Análises de paleotensões identificam três pulsos de deformação, destacando a complexidade da evolução da paisagem em regiões

intraplacas. Essas descobertas ampliam o conhecimento sobre a tectônica regional, ressaltando a necessidade de compreender a evolução das paisagens em áreas interiores de placas, como a Sul-Americana.

Palavras-chave: Geomorfologia Tectônica; Evolução da Paisagem; Índices Geomórficos; Tectônica Rúptil.

1. Introduction

Tectonic movements at plate boundaries can reactivate large preexisting geological structures in intraplate continental regions (ZOBACK, 1992), through process-response mechanisms that act in the geomorphological landscape sculpting. In this sense, tectonic geomorphology plays a role in the analysis and identification of signatures in topography and drainage networks, using geomorphic indices to evaluate the morphotectonic controls of the terrain (KELLER; PINTER, 2002; BULL, 2007; BURBANK; ANDERSON, 2011; KIRBY; WHIPPLE, 2012). Unlike active orogenic areas, intraplate continental regions tend to exhibit low rates of tectonic activity (STAIN; MAZZOTTI, 2007). In this aspect, the continental interior of the South American Plate is considered tectonically the least active of all intraplate regions globally (AGURTO-DETZEL et al., 2017; CAMPOS et al., 2023).

Over the last few decades, several studies have focused on the Cenozoic tectonics of various Brazilian regions (e.g. RICCOMINI, 1989; 1995; FERNANDES; AMARAL, 2002; SALAMUNI et al., 2004; CHAVEZ-KUZ; SALAMUNI, 2008; FRANCO-MAGALHÃES et al., 2010; NASCIMENTO et al., 2013; PEYERL et al., 2018; PINHEIRO et al., 2019; SANTOS et al., 2019a; PINHEIRO; CIANFARRA, 2021; SILVA; FURRIER, 2019; FURRIER; SILVA, 2020; CALEGARI et al., 2021; FURRIER; SILVA, 2021; SILVA et al., 2021; FARIAS et al., 2022; GIMENEZ et al., 2022; SANTOS et al., 2022; SANTOS et al., 2023), aiming to delineate the evolutionary framework of deformational events occurring since the Cretaceous, a temporal milestone of the last substantial tectonic event in the region, linked to the breakup of Western Gondwana. The Paraná Sedimentary Basin, considered one of the main geotectonic units in Brazil, has been subjected to successive deformational events since the Paleozoic, associated with tectonic interaction in the plate margin regions around it. Extensive zones of Proterozoic basement faults, derived from the Brasiliano orogeny, have been reactivated throughout the basin's history, conditioning its tectonostratigraphic evolution (ZALÁN et al., 1990; MILANI; RAMOS, 1998; SOARES et al., 2007). It is reasonable to consider that tectonic events or pulses recorded in the marginal taphrogenic basins of southern and southeastern Brazil, including those neotectonic, may be related to tectonic disturbances within the Paraná Basin. In this aspect, topography and drainage systems may gather important records of this probable relationship, as there is a strong connection between their dynamic adjustment and the balance between uplift and erosion rates (e.g.; KIRBY; WHIPPLE, 2012). Thus, by combining geomorphic analysis with tectonostructural analysis, it is expected to advance in understanding how tectonic control occurs under low deformation rates in intraplate continental landscapes. Evidence of such a relationship is a gap in the intraplate context of this region, as substantial tectonic activity ceased several tens of millions of years ago. This work investigates this hypothesis in the surroundings of Londrina (PR), a relatively restricted area within the Paraná Basin, but which has shown recent low-magnitude seismic activity.

The study area is in the northern part of the state of Paraná (Figure 1). Recent seismic activity was recorded in the area from 2015 to 2018, with magnitudes between 0.8 and 2.1 degrees on the Richter scale, according to data released by the Seismology Center of USP – IAG/IEE (Figure 1C). In the region, the Eocretaceous basalts of the Serra Geral Group outcrop, inserted in the Paraná Igneous Province, which record an intricate network of joints and subvertical faults, serving as temporal markers for the history of brittle deformation that occurred in the Paraná Basin from the Cretaceous to the Cenozoic. The area is under the influence of the Ponta Grossa Arch, developed in the process of Western Gondwana breakup and opening of the South Atlantic. It is in a geological domain close to the São Jerônimo-Curiúva lineament and the Guaxupé fault, local representatives of the inherited structuring of the Proterozoic basement (FERREIRA, 1982; ZALÁN et al., 1990) and with indications of Cenozoic reactivation (SANTOS et al., 2022; SANTOS et al., 2023).

The main objective of the study is to determine the post-Cretaceous tectonic regime that would have acted in this portion of the basin, focusing on possible reactivations along the São Jerônimo-Curiúva Lineament and other subsidiary structures, and their potential reflection on landscape dynamics. This study contributes to advancing the understanding of brittle deformation events and Cenozoic morphotectonics in the Paraná Basin, as well as adding insights into the understanding of interactions between tectonics and surface processes at the geodetic level in the intraplate continental interior of the South American Plate.

2. Geological and geomorphological context

The geological context of the surroundings of the municipality of Londrina, in the northern state of Paraná (Figure 1A, B), is dominated by Eocretaceous-age basalt rocks from the Serra Geral Group, belonging to the Gondwana III Supersequence of the Paraná Sedimentary Basin (MILANI et al., 2007). These magmatic rocks were generated by intracontinental fissure volcanism events associated with the Gondwana fragmentation process, resulting in the overflow of the Paraná Igneous Province (PIP) (GOMES et al., 2018). The Serra Geral magmatism (Figure 1B), dated to the Eocretaceous (134 Ma – THIEDE; VASCONCELOS, 2010), produced about 600,000 km³ of volcanic rocks (FRANK et al., 2009), predominantly tholeiitic basalts (90%) (BELLIENI et al., 1986). In the Londrina region, basalt to andesite-basalt rocks enriched in Fe_2O_3, MgO, and TiO_2 are found, which, according to Licht (2016), are representative of the Central-North sub-province of PIP and exhibit an intricate network of fractures.

The area is intersected by the São Jerônimo-Curiúva Lineament and the Guaxupé Fault (Figure 1B). These structures play a significant role in the context of tectonic reactivation processes in the brittle deformation history that occurred in the Paraná Sedimentary Basin since the Cretaceous.

The main tectonic structures of the Paraná Sedimentary Basin correspond to significant alignments in the NE-SW and NW-SE directions (SOARES et al., 2007), related to pre-existing structures in the basin itself that determined its evolution. The NE-SW direction reflects strong structuring of the Brasiliano basement, represented, for example, by the Guaxupé and Taxaquara faults, and the NW-SE direction results from the orientation of structures that delineate the Ponta Grossa Arch (APG) related to continental rifting, such as the Curitiba-Maringá, São Jerônimo-Curiúva, and Guapiara lineaments (ZALÁN et al., 1990). According to Ferreira (1982), the APG has been active since the depositional onset of the Paraná Basin, structurally conditioning the basin's sedimentary units, i.e., it would have acted throughout the tectonostratigraphic evolution of the basin, functioning as zones of intraplate stress accommodation and dissipation (ZALÁN et al., 1990). In the arch's evolution, two extensive swarms of NW-SE diabase dikes are formed, the Curitiba-Maringá Lineament coinciding with the hinge, and the Guapiara Lineament positioned at the northern edge of the arch. Subordinately to the NE-SW and NW-SE directions, E-W alignments occur, such as the São Sebastião Lineament, corresponding to the Paranapanema Direction (SOARES, 1991), being well recognized in Quaternary deposits along the Paraná Basin (SOARES et al., 2007).

At the end of the Jurassic and the beginning of the Cretaceous, concurrently with the Gondwana breakup for the opening of the South Atlantic Ocean, the third subsidence phase occurred in the Paraná Sedimentary Basin (ZALÁN et al., 1990). This interval was marked by both the overflow of lavas from the Paraná Igneous Province (PIP) and the Jurassic-Cretaceous reactivation of old basement structures, resulting in tectonic responses in various structural representatives. According to Barcelos (1984), tectonic activities related to the activation of the APG at the end of the Mesozoic were responsible for a subsidence of the Brazilian Platform to the west and southwest. The study area is intersected by the São Jerônimo-Curiúva Lineament, the Guaxupé Fault at its southwest extremity, and the São Sebastião Lineament in its southern portion (Figure 1B).

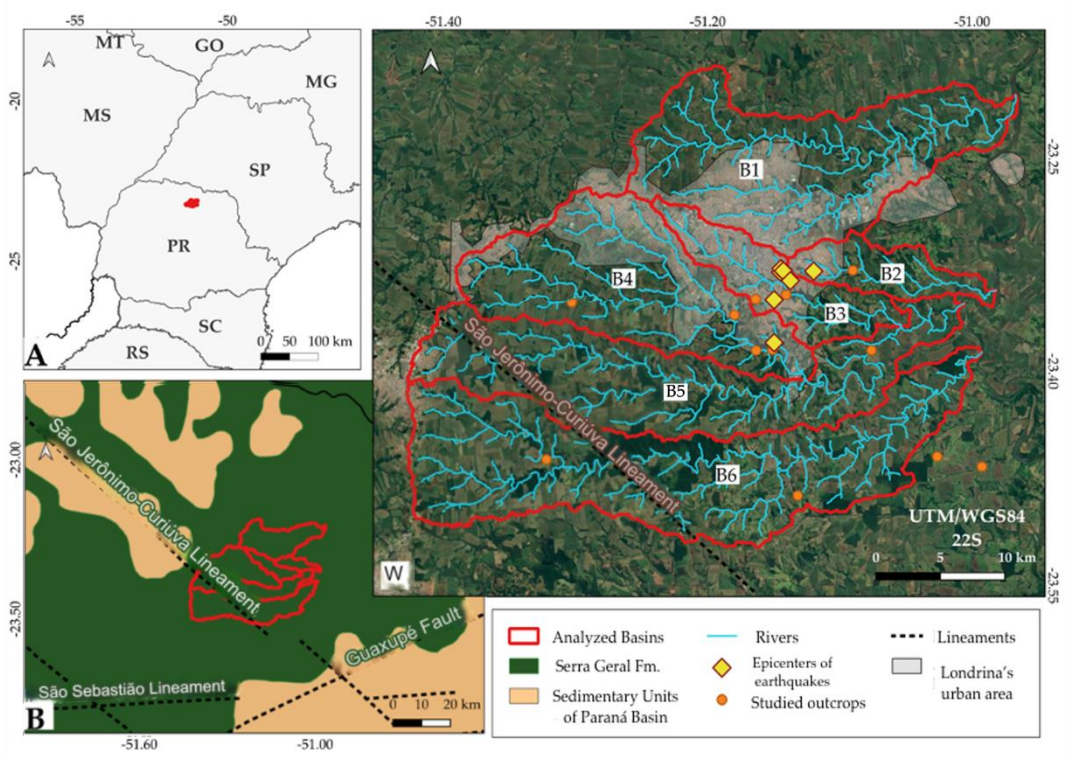

Figure 1. Location map of the study area, showing the geological-structural context, highlighting the fourth-order hydrographic basins analyzed (B1, B5, and B6, respectively, Jacutinga, Três Bocas, and Apertados basins), the Limoeiro basin (B2), and the sub-basins of B5 (B3 and B4, Cambé and Cafezal respectively). The orange points indicate the studied outcrops, and the yellow points indicate the epicenters of earthquakes recorded between 2015 and 2018.

The geomorphological compartmentalization of the studied region is part of the morphostructure of the Paraná Sedimentary Basin, belonging to the morpho-cultural unit of the Third Paraná Plateau (SANTOS et al., 2006). This unit, resulting from the sculpting process due to extensive volcanic eruptions of basic eruptive rocks, covers approximately two-thirds of the territory of Paraná and manifests morphologically as a series of flat elevations, predominantly sloping towards the west-northwest. The post-Cretaceous evolution of the basin, associated with the uplift of marginal mountain ranges and marginal denudation processes, sculpted systems of cuestas and steep plateaus in the landscape (BARTORELLI, 2004).

Specifically, the study area falls within the domains of the Londrina Plateau, a sector characterized by moderate dissection relief, marked by elongated hilltops and convex slopes, with river valleys in "V" shapes, preferentially entrenched in the fractures of basaltic rocks. Concerning the fluvial geomorphology of the study area, it is conditioned by the hydrographic basin of the Tibagi River, a typical rocky-bed river and an important tributary of the left bank of the Paranapanema River, flowing in a north-south direction. The Tibagi River constitutes an antecedent drainage to the processes generating regional landforms and follows, in a concordant manner, the dip of the units of the Paraná Basin. The main rivers in the study area, whose basins were chosen for research, are tributaries on the left bank of the Tibagi River.

3. Materials and methods

3.1. Background

In erosional regions dominated by bedrock rivers (c.f. WHIPPLE; TUCKER, 2002), such as the case of the study area, the balance between uplift rate (U) and erosion rate (E), that is, U-E, determines the long-term landscape dynamics (HACK, 1960; HOWARD, 1965). The ideal of long-term spatiotemporal topographic equilibrium, equalizing both rates and consequently maintaining constant mean elevation over time, is unlikely in nature (WILLETT; BRANDON, 2002), including in intraplate interiors under low tectonic activity (e.g. CAMPOS et al., 2023). This is due to the diversity of external and internal disturbing factors (e.g., climate, tectonics, reorganization of river basins, and lithology), their combinations and interconnections, and the dynamics of boundary conditions.

Previous studies (e.g. WHIPPLE; TUCKER, 1999; 2002) based on the stream power model (HOWARD; KERBY, 1983) reveal a direct relationship between channel morphology/incision and the balance between uplift and erosion rates, signaled through adjustments of the longitudinal profile. The stream power model demonstrates a positive relationship between channel slope and uplift rate, as well as with precipitation and lithological strengt (cf. PEIFER; CREMON; ALVES, 2020). Therefore, when crossing a zone of higher uplift rate/base level fall or disparate precipitation or even more resistant lithologies (lower erodibility), the channel will increase its local gradient and consequently its incision, creating a sudden convexity (knickpoint) in its originally concave profile (e.g. WOLPERT; FORTE, 2021). The knickpoint thus marks a channel adjustment, by increasing incision, in response to a change, and when collectively concentrated in similar elevations (cluster of slope-break knickpoints) indicate a common change in boundary conditions, such as regional uplift/base level fall (e.g. KIRBY; WHIPPLE, 2012).

Along reactivated faults marking different uplift rates, the increase in local channel slope occurs towards the zone of higher uplift rate. Consequently, the analysis of channel slope contrasts can provide important clues for understanding landscape evolution and its relationship with controlling factors in regions of low tectonic activity, such as intraplate regions. The normalized channel steepness (*ksn*) (c.f. PEIFER; CREMON; ALVES, 2020) is a robust metric of channel gradient, normalized for different drainage areas, widely used to identify, and analyze disturbances in landscape dynamics, presenting a positive relationship with denudation and uplift rates (KIRBY; WHIPPLE, 2012). Since the *ksn* varies according to the channel concavity index (θ), it is necessary to calculate the best reference value of θ for basins of different areas (WOBUS et al., 2006; MUDD et al., 2018). Contrasting values of *ksn* can indicate lithological contrast, climatic or uplift variations, and fault reactivations (e.g., BOULTON et al., 2014; CAMPOS et al., 2023). For example, rivers flowing transversely to a reactivated fault zone will exhibit knickpoints aligned with the structure direction, regardless of their elevations, and migrating towards the sector of higher uplift rate and the most active segment (e.g., WOBUS et al., 2006; BOULTON et al., 2014). Additionally, channel longitudinal profiles will present segments with steeper gradients associated with the zone of higher uplift.

Recently, the analysis of river longitudinal profiles has gained robustness through the integral analysis method or chi analysis (PERRON; ROYDEN, 2013) and the use of *chi*-plots (*chi*-elevation space), with consideration, in comparative analyses, of the same reference drainage area (A0) and the same θ value for all analyzed rivers. Under conditions of dynamic equilibrium (U=E) and uniform lithology, *chi*-plots appear linear with collinear rivers, with the profile slope in elevation-chi space representing the *ksn* index. Therefore, it is possible to estimate whether the area is in dynamic equilibrium or not, and the proportion of uplift, erodibility, and precipitation, and if there is spatial variation of these in the area through visual analysis of *chi*-plots (PERRON; ROYDEN, 2013). Additionally, *chi*-plots combined with knickpoint extraction allow for the detection of widespread uplift or base level fall events, signaled by a concentration of knickpoints in a narrow chi range or even at a specific value (PERRON; ROYDEN, 2013), since the vertical migration rate of slope-break knickpoints (cf. WOBUS et al., 2006) is constant (WHIPPLE; TUCKER, 1999).

For a consistent analysis of the topographic dynamics of a landscape and its controlling factors, it is also necessary to analyze whether the watershed divides are in a state of equilibrium (WILLET et al., 2014). This is because the area of the watershed directly influences the capacity and speed of incision of the rivers composing it and, consequently, the configuration of the longitudinal profiles of the rivers, disturbing *ksn* values and the shape of profiles in elevation-chi space, since the flow, expressed by the drainage area upstream, is one of the parameters for calculating the channel slope (FLINT, 1974). In this sense, substantial changes in the area of the watershed through captures and divide migration, triggered by tectonics, climate, or lithological contrast, or a combination of these, can interfere with the topographic dynamics (WHIPPLE et al., 2016). This geometric and topological rearrangement of drainage has long been of interest (e.g. DAVIS, 1889; BISHOP, 1995), and recent studies have contributed to its better understanding with metrics for calculating the direction and migration rate of the divide (e.g., WILLET et al., 2014; WHIPPLE et al., 2016; BEESON et al., 2017). A watershed gaining upstream drainage area undergoes an increase in *ksn* and acceleration of erosion/decrease in chi values, while the watershed losing drainage area decreases ksn/increases chi values (WILLET et al., 2014). Therefore, the greater the contrast of *ksn* and chi transversely to the divide, the higher the mobility rate of it, and the divide migrates towards the sector of higher chi/lower *ksn* (WILLET et al., 2014; WHIPPLE et al., 2016). The erosion acceleration by the aggressor watershed is the mechanism to restore the longitudinal profile equilibrium and stabilize the mobility of the divide (WHIPPLE et al., 2016). The analysis of the spatial distribution of *chi* and *ksn* through chi maps (WILLET et al.,

2014) and *ksn*, therefore, can reveal whether the divides are stable or migrating, indicating the condition of topographic dynamics.

Thus, topographic metrics and longitudinal river profiles collectively can encapsulate signals of changes or disturbances in the landscape triggered by combined or isolated controlling factors (e.g., KIRBY, WHIPPLE, 2012), constituting valuable indicators of landscape evolution and controlling factors in intraplate contexts. In this regard, quantitative geomorphic analysis based on DEMs (e.g., PEIFER; CREMON; ALVES, 2020; CREMON et al., 2022) combined with tectono-structural analysis can provide clues for understanding the dynamics and evolution of the landscape under low rates of tectonic activity (e.g. CALEGARI et al., 2021; SANTOS et al., 2023), whose complexity is still minimally understood (e.g. GALLEN; THIGPEN, 2018).

3.2. Geomorphic analysis

We explored spatial variations in topographic patterns, adjustments of the longitudinal profiles of the main rivers in the area, and the dynamics of their basins and divides, seeking signs of disturbance and possible relationships with the area's main tectonic structures. To do so, we initially built a database using the Copernicus Digital Elevation Model (DEM) (SINERGISE, 2021) with spatial resolutions of 90 m and 30 m (COP 90 m and 30 m), available on OpenTopography (https://opentopography.org/) and reprojected to WGS 1984 UTM Zone 22S. The choice of the COP-30 DEM (second arc) was due to its excellent vertical accuracy (1.98 m; CREMON et al., 2022), performing better than LiDAR and free global DEMs (ALOS, ASTER, NASA, and SRTM) for both high and low slope areas (PURINTON; BOOKHAGEN, 2021), ensuring higher quality in landscape representation and topographic analysis (GUTH; GEOFFROY, 2021).

For the analysis of topographic metrics, using the COP 30 m DEM, hypsometric and slope maps were processed in ArcGIS software (version 10.5; ESRI, 2016), overlaid with a 50% transparency *hillshade* map for terrain characterization and identification of altitude and pattern contrasts. The *hillshade* map was generated with an Azimuth of 40° and vertical exaggeration (Z) of 5.0x. Relief lineaments were extracted on a 1:80,000 scale from the DEM with shading. Using the COP DEM 90 m, we established the base level at 230 m encompassing the Paranapanema basin area and extracted the 4th order basins, estimating the best θ value (~0.45) using the MATLAB software with the "*mnoptimvar*" algorithm from the TopoToolbox, derived from the "robustcov" function (HERGARTEN et al., 2016). With the base level at 230 m, θ value of 0.45, and a minimum area of 1 km², we computed the normalized channel steepness index *(ksn*) and chi by the integral method (PERRON; ROYDEN, 2013) for all channel segments using the "*KsnChiBatch*" function of the Topographic Analysis Kit TAK (FORTE; WHIPPLE, 2019). To create a detailed chi map for the area, we resampled the data extracted from the COP DEM 90 m to a 30 m resolution. *Ksn* was processed from the COP DEM 30 m using the "KsnChiBatch" function and a 1000 m smoothing window. For knickpoint extraction in the study area, we first calculated the tolerance (12.57) using the Constrained Regularized Smooth (CRS) technique (SCHWANGHART; SCHERLER, 2017) to avoid false knickpoints generated by artifacts of the COP DEM 30 m. Then, establishing the tolerance at 13 m, knickpoints were extracted for all channels in the study area using the "knickpointfinder" algorithm with a minimum drainage area threshold of 1 km² after processing the "quantile carving" algorithm with a 0.5 quantile in the TopoToolbox (SCHWANGHART; SCHERLER, 2017).

To investigate signs of disturbances in river longitudinal profiles, we selected the 4th order hydrographic basins B1, B5, and B6 as they are more representative of the study area, in addition to the Limoeiro hydrographic basin, containing one of the recent seismic epicenters (Figure 1). We explored channel behavior in distance-elevation and chi-elevation space (chi-plots) combined with extracted knickpoints using the "chitransform" algorithm in the TopoToolbox, with a minimum drainage area threshold of 1 m², a value of 0.45 for θ, and a tolerance of 13 m for all basins.

Additionally, drainage asymmetry factors (AF – HARE; GARDNER, 1985) and transverse topography factors (T - COX, 1994) were calculated for the four hydrographic basins (Jacutinga - B1; Limoeiro - B2; Três Bocas - B5; Apertados - B6) and the two sub-basins of the Três Bocas Basin (Cambé B3; Cafezal B4). The results could be used to infer basin tectonic tilting (e.g. SANTOS et al., 2019b). Using the routines proposed by Harbor et al. (2005), a knickpoint distribution map was generated for the study area. Elevation data from the digital elevation model were plotted on a logarithmic scale for graphical representation of the channels.

3.3. Tectono-Structural analysis

For the analysis of tectonic activity, the most prominent brittle structures (faults and joints) in the area were surveyed and analyzed through a study of their geometry and kinematic indicators in the field. These data were organized and processed using the right dihedral method (ANGELIER, MECHLER, 1977) with the assistance of the Wintensor software v.9.5.1 (DELVAUX, SPERNER, 2003; http://damiendelvaux.be/Tensor/ WinTensor/win-tensor.html), aiming to determine the paleostress responsible for regional tectonic deformation.

4. Results

4.1. Topographic configuration

The altimetric configuration of the studied area corresponds to maximum altitudes of ~875 m (Apertados basin - B6) and minimums of ~330 m (Jacutinga basin - B1) (Fig. 2A). The results show strong topographic asymmetry in the area, with the highest elevations concentrated in the western sector, coinciding with the main N-S oriented watershed that delimits the western edge of the Tibagi River basin in this portion (Fig. 2A), dividing the watersheds of the Tibagi River to the east and Pirapó River to the west. This high plateau, oriented N-S, is dissected by straight river valleys, entrenched in fractures and faults of the bedrock, preferably oriented E-W and NW-SE. After sustaining the headwaters of the Apertados basin in the south of the area, the watershed inflects to NE-SW, descending in altitude to the north and northeast where it marks the division of the watersheds of the Tibagi River to the east and Ribeirão Vermelho to the west, the latter flowing parallel to the former. The secondary watersheds to the main watershed, which delimit the main tributary basins of the Tibagi River on the left bank, are roughly oriented around the E-W direction, descending to the east to varying degrees between the 4th order basins, following the natural slopes of the Tibagi River basin. The southern slopes of the E-W watershed dividers of the Apertados and Três Bocas basins are steeper than the northern faces, with this asymmetry attenuated towards the north of the area (E-W divider between Três Bocas and Jacutinga and between this and the adjacent basin to the north) (Figs. 2A, C).

The terrain presents a significant level of dissection, with less pronounced slopes and remnants of narrow, flattened high points in the western/northeastern portion contrasting with the more excavated and topographically lower portion near the Tibagi valley bottom. Slopes increase to the east, especially in the transition from the middle to the lower reaches of the 4th order basins - B1, B5, and B6 (Fig. 2C). Downstream of this transition, increases in channel sinuosity (meandering) and widening of river valleys towards the confluence with the main river are observed. A steep escarpment with N50-60E direction is noticeable, marked by breaks in the profiles of the main channels and increased slope of the slopes coinciding with this transition (Fig. 2C). Knickpoints are distributed in the area, especially demarcating the NW edge of the N50-60E escarpment and upstream of it (Figs. 2A, B, C).

The *ksn* values range from 0 to 56.8 $m^{0.9}$, with the lowest values in the Jacutinga basin and the highest along the main river (>42 $m^{0.9}$) in the southeastern sector of the area (Fig. 3). The results also point to high *ksn* values along the NE-SW escarpment, contrasting with the upstream and downstream stretches with low values. It is also noted that the mouth of the Limoeiro basin deviates from the *ksn* pattern of the other basins, contrasting with a longer stretch of higher values near the mouth, although all show an increase in *ksn* near the confluence with the Tibagi River. The results also show stretches with contrasting *ksn* in channels along the São Jerônimo-Curiúva Lineament in the western sector of the area (Figs. 1 and 3). The Jacutinga basin presents the smallest contrasts in *ksn* compared to the other basins analyzed, coinciding with the stretch of the main river with the lowest values as well.

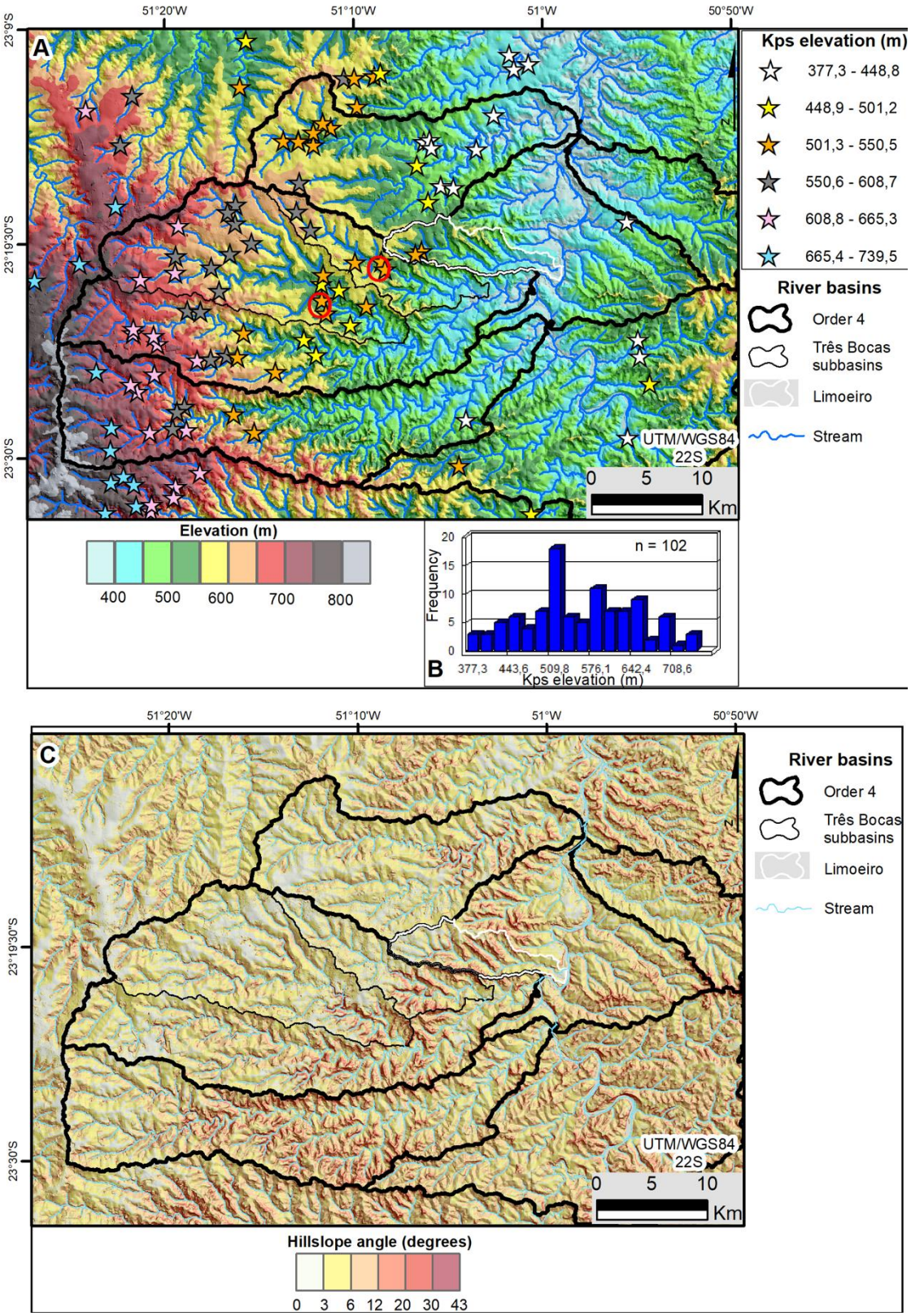

Figure 2. Topographic configuration of the study area. (A) Hypsometric Map and spatial distribution of knickpoints (*Kps*) - red circles indicate *kps* with greater height (dz) (~50 m) in the area; (B) Elevation Histogram of Knickpoints (above sea level) and frequency for all extracted knickpoints (mean = 559.4; median = 550.6; standard deviation = 87.59; Coefficient of variation = 15.7%; kurtosis = -0.7); (C) Slope Map overlaid on shaded image.

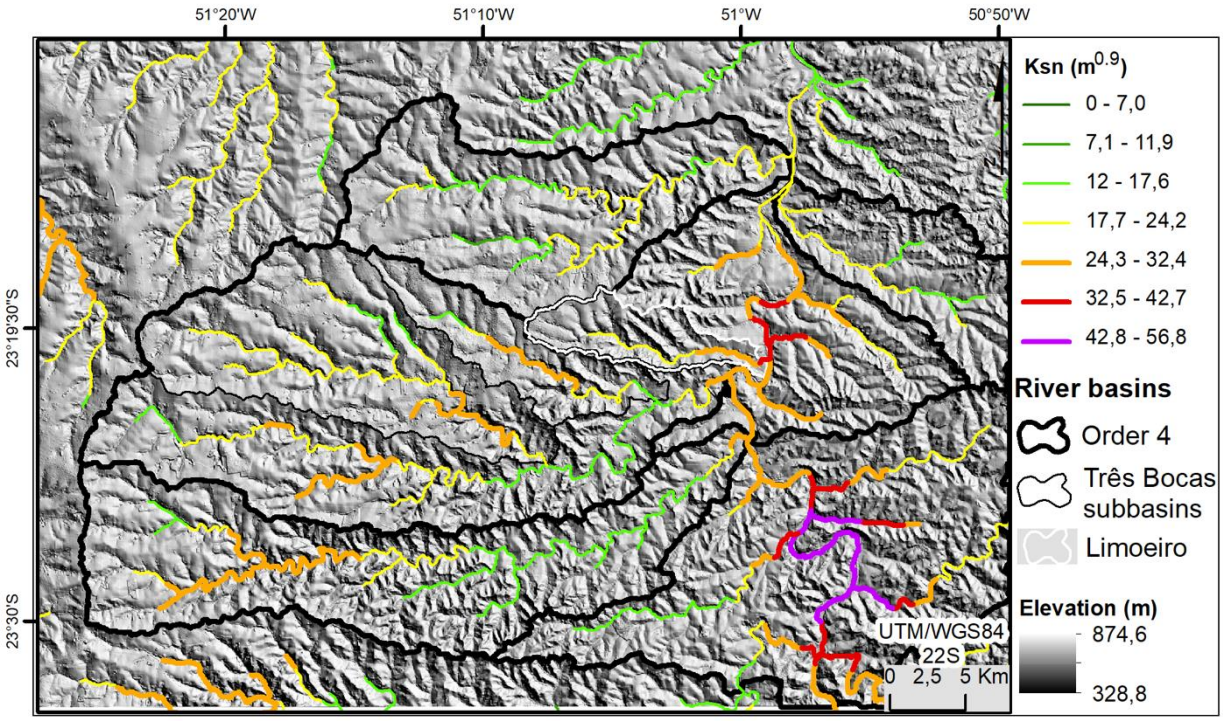

Figure 3. Map showing the spatial variation of the normalized slope index (*ksn*). Highlighting the high ksn values along the Tibagi River in the southeastern portion of the area.

4.2. Analysis of the drainage network

The drainage network of the study area includes a stretch of the Tibagi River, an important tributary on the left bank of the Paranapanema River, constituting an extensive basin with a general north-south direction. In addition to the Tibagi River, most of the area is drained by its left bank tributaries, notably the Jacutinga, Limoeiro, Três Bocas Stream, and its two main tributaries - Cambé Stream and Cafezal Stream - and the Apertados Stream (Fig. 4). The headwaters of the rivers are located to the west, in the elevated regions of the Londrina Plateau (SANTOS et al., 2006). The valleys and interfluves of the main channels predominantly have orientations in the E-W and NW-SE directions, forming elongated ridges and valleys aligned in this direction. The channels flow to the east, with inflections to the northeast in the lower course until the mouth, except for the Limoeiro River (Fig. 4).

Rocky-bed channels dominate the area, with a small area of alluvium on the banks. The E-W and NW-directed channels are more extensive compared to those in the NE and N-S directions.

Dendritic and sub-dendritic patterns predominate, along with the marked presence of parallel, rectangular, and trellis patterns, evidencing tectonic control of drainage. Anomalous meanders in the transition to the lower course, compressed meanders, as well as elbows, are geomorphic elements that may indicate tectonic influence (SCHUMM et al., 2000) and are noted in the analyzed basins (Fig. 4).

The drainage network exhibits 102 knickpoints (Figs. 2A, B) at elevations ranging from ~380 m to ~740 m (Fig. 2A, B) and heights between ~50 and 13 m, with the two knickpoints with the greatest height (49.7 m and 48.3 m) located in the sector of seismic epicenters in the sub-basins of the Três Bocas Basin (Cambé and Cafezal), one of them exactly coinciding with an epicenter in the Cambé sub-basin (Figs. 1C and 2A). The distribution of knickpoint elevations is almost normal, with the mean (559.4 m) very close to the median (550.6 m), indicating a slight positive asymmetry, i.e., a slight tendency to concentrate at elevations slightly below the average and few knickpoints at discrepant elevations on the highest ridges. The dispersion is weak, indicated by a low coefficient of variation (15.7%) and kurtosis close to 0 (-0.7). It is observed that knickpoints predominantly occur from the N50E escarpment, demarcating its northwest edge. Knickpoints with lower elevations are concentrated in the Jacutinga basin and north of it. It is also noted that knickpoints are less evident along the main river and in the middle and lower reaches of the Apertados and Limoeiro basins. The results show a tendency for concentration of greater knickpoint heights along the NE-SW escarpment, coinciding with the strip of higher slope and contrasting *ksn* (Figs.

2, 3, and 5). In contrast, knickpoints at higher elevations predominantly have low heights, rarely exceeding 22 m (Figs. 2A and 5).

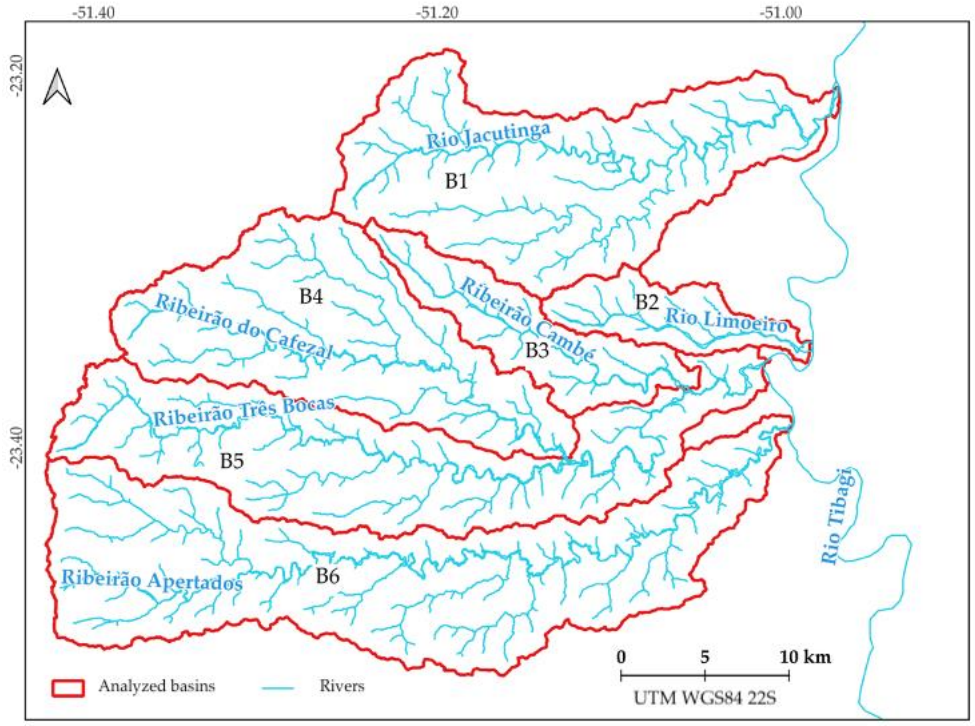

Figure 4. Drainage network of the study area highlighting the analyzed basins.

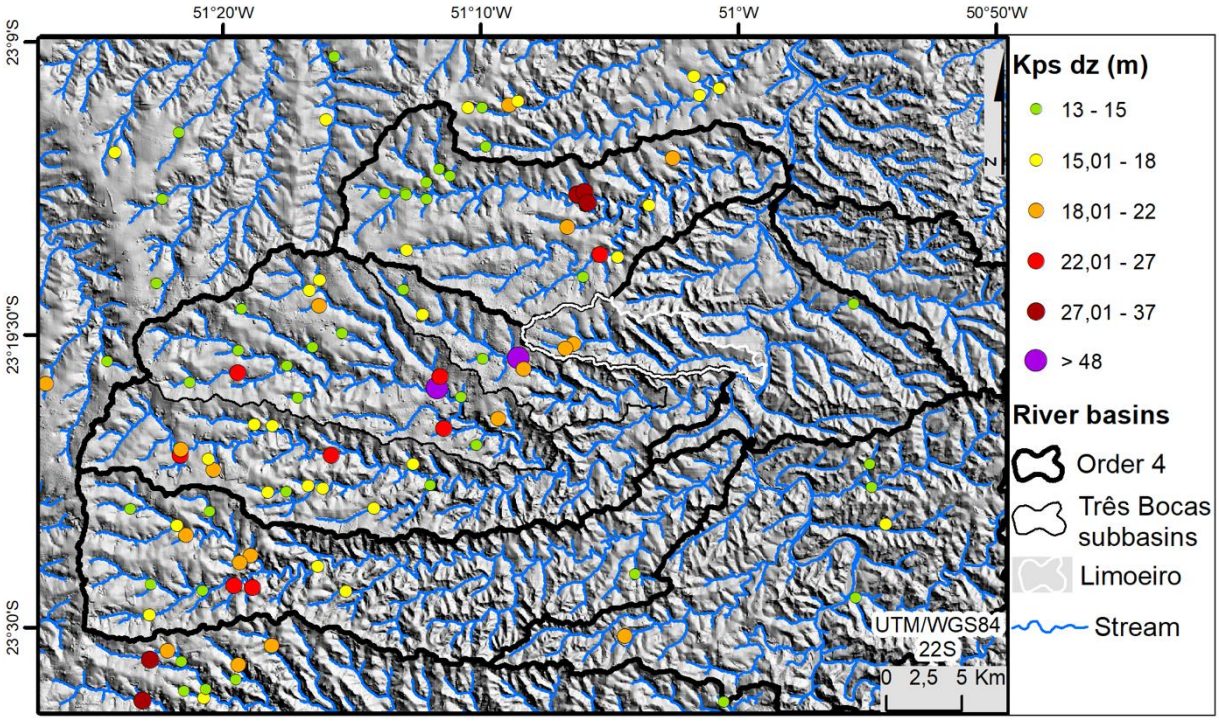

Figure 5. Spatial distribution of knickpoints and their heights (*dz*) in the area.

The spatial distribution of *chi* for the area indicates that the N-S stretch of the main divide is symmetric on both the east and west faces, although the eastern slope shows a greater advancement of the incision front (Fig. 6). However, upon inflecting to the NE, it becomes asymmetric, migrating to the NW, indicating an increase around

the Três Bocas basin through the capture of the headwaters of the Ribeirão Vermelho watershed in the northwest portion of the area. The secondary E-W divides tend to migrate to the north and northeast, expanding the northern flank of the Três Bocas and Apertados basins. On the southern flank of the Apertados basin, the trend reverses, and the divide migrates southward, indicating that it tends to expand its area on both flanks, capturing the headwaters of the adjacent basins to the north (Três Bocas basin) and south. There is also a segment in imbalance in the divide between the Cambé and Cafezal sub-basins coinciding with one of the tallest knickpoints and near seismic epicenters (Figs. 1 and 6).

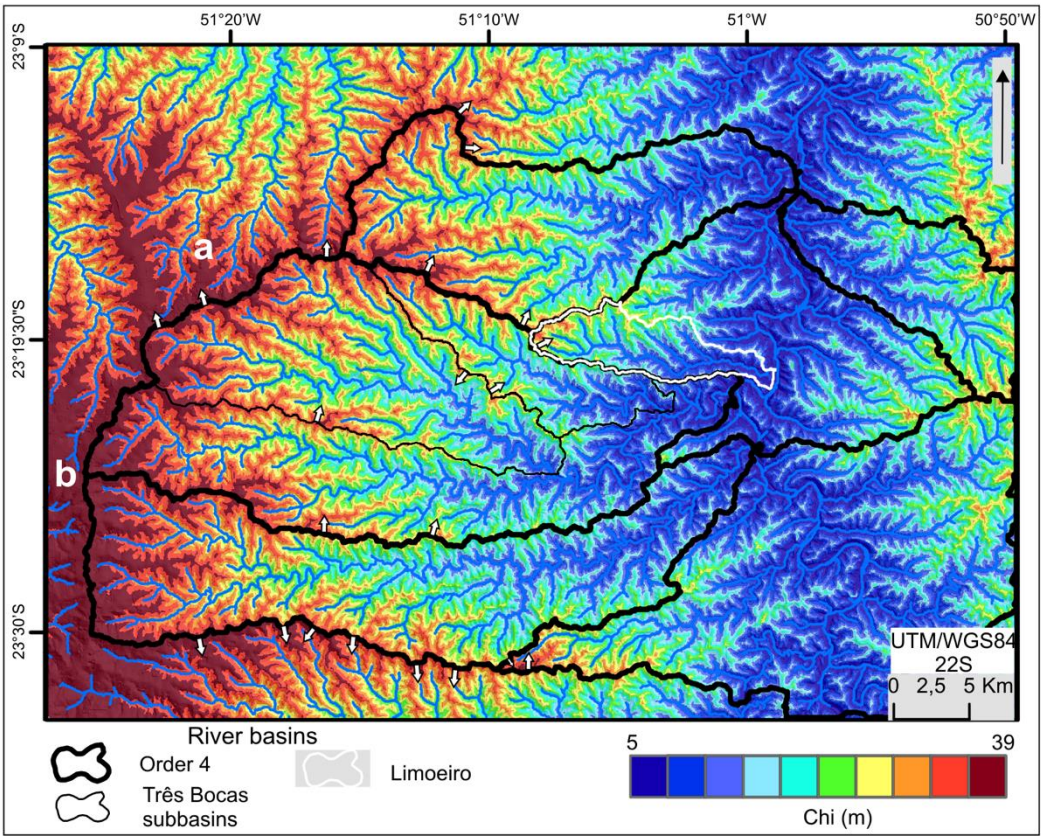

Figure 6. *Chi* map and migration of divides between the main hydrographic basins in the area. (a) and (b) are respectively the basins of Ribeirão Vermelho and Pirapó respectively. The white arrows indicate sectors of the divide in imbalance and the direction of its migration.

Regarding the asymmetry factor of the analyzed basins, the Apertados River basin, at the southern extreme of the area (B6), has the highest asymmetry factor value (AF = 71.5), with asymmetry towards the left bank, indicating tilting and channel migration to the north (Fig. 7). Similarly, at the northern extreme of the area, the Jacutinga River basin (B1) also shows tilting to the north, with an AF value of 61.5. In contrast, the other basins show tilting and trunk migration to the southern quadrant, with the Limoeiro River basin (B2) exhibiting an AF value of 33.6, and the Três Bocas River basin (B5), 28.16. The basins of its tributaries, the Cafezal and Cambé rivers, also showed tilting towards the right bank (south), although with more subtle values of the asymmetry factor compared to the other analyzed basins.

The calculations defined by Cox (1994) for the determination of the transverse topographic symmetry factor (T) involved the sectorization of each analyzed basin for a more detailed analysis that considered the particularities and inflections of the main channels, which do not behave uniformly along their course. Each basin was analyzed in five approximately equidistant sections from the headwaters to the mouth. T values close to 0 would indicate basins (or sections) with symmetric characteristics, not tilted, while increases in the value of T, approaching 1, would indicate asymmetrical basins and/or sections, indicating tilting. We considered T values > 0.5 as markedly asymmetrical sections.

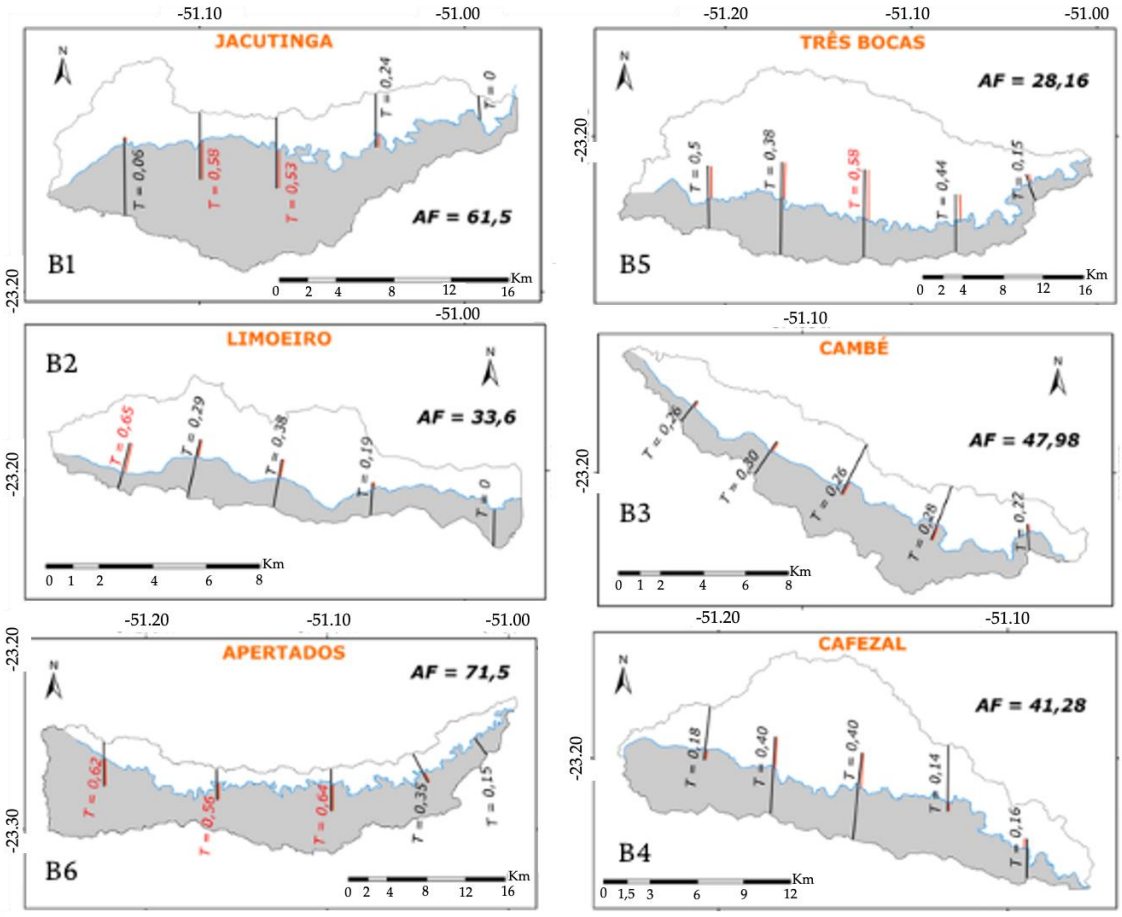

Figure 7. Asymmetry Factor (AF) and Transverse Topographic Symmetry Factor (T) of the six analyzed hydrographic basins.

In all analyzed basins, we observed a decrease in the values of T from the headwaters to the river mouth. In the Apertados River basin, the highest number of markedly asymmetric sections was recorded from the headwaters to its median portion. The Limoeiro River basin recorded a single markedly asymmetric section, in the region near the headwaters. In the Jacutinga and Três Bocas river basins, the asymmetric sections were located in the median portions of the basins, while the Cambé and Cafezal river basins showed the lowest values for the transverse topographic symmetry factor.

The Apertados River basin is asymmetric to the north, from the upper to the middle course, while the Três Bocas basin records more asymmetric values in portions of the middle course, with asymmetries to the south. The Cafezal and Cambé basins showed asymmetry to the south, following the general tilting of the Três Bocas River basin (Figs. 7 e 8). The Limoeiro River basin recorded tilting to the south, with a high T value near the source and values indicating greater symmetry gradually towards the mouth of the main channel. The Jacutinga River basin showed little tilting in the initial section but recorded increases in the T factor in portions of the middle course, decreasing again towards the mouth of the main channel in the Tibagi River.

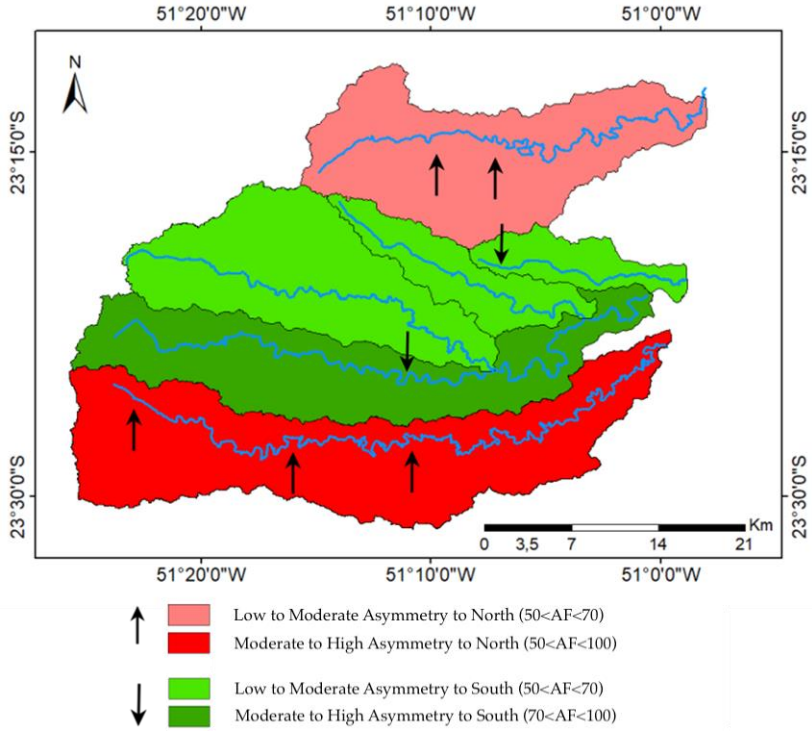

Figure 8. Schematic map representing the potential tilting of drainage basins: shades of red indicate tilting towards the north, while shades of green indicate tilting towards the south, considering the values of AF; arrows indicate the sections in each basin associated with more pronounced asymmetries (T > 0.50).

4.3. Analysis of river longitudinal profiles

The main rivers analyzed exhibit longitudinally imbalanced profiles in general (Figs. 9 and 10), with gradient breaks marked by clusters of knickpoints predominantly in the upper course (Figs. 9B; 10B) or middle and upper courses (Figs. 9A, C, D; 10A, C, D). Although the results reveal a certain degree of knickpoints scattering, especially in the Três Bocas basin (Figs. 9C and 10C), a common knickpoint cluster is noted around 500 to 550 m elevation and a range of chi values between ~4000 and 6000 m, corroborating the statistics presented in Figure 2B indicating a higher knickpoint frequency between 500 and 550 m elevation. Interestingly, the Três Bocas and Apertados basins reveal another knickpoint cluster at elevations between 650 and 700 m with chi values around ~8000 m (Figs. 10c,d). There is an increase in slope downstream from the highest knickpoint concentrations in the chi-transformed profiles of all analyzed basins (Fig. 10), with a more pronounced degree in the Três Bocas basin (Fig. 10c). The total incision, visually estimated from the *chi*-elevation profiles (KIRBY, WHIPPLE, 2012), varies among the basins, around 150 m in the northern portion basins (Jacutinga and Limoeiro; Figs 10 A, B), and around 300 m in the southernmost basins (Três Bocas and Apertados; Figs. 10C, D). The chi-elevation profiles exhibit some non-collinear tributaries in the studied basins, except for the Limoeiro basin containing a strong collinearity with the tributaries (Fig. 10). The patterns of the basins near the mouth vary between oscillatory (Fig. 10C) and increased gradient (Figs. 10B, D). There is also a contrast in the slope pattern of the headwater sector among the analyzed basins, marked by a decrease in slope in the Limoeiro basin while the others maintain high slope (Figs. 9 and 10).

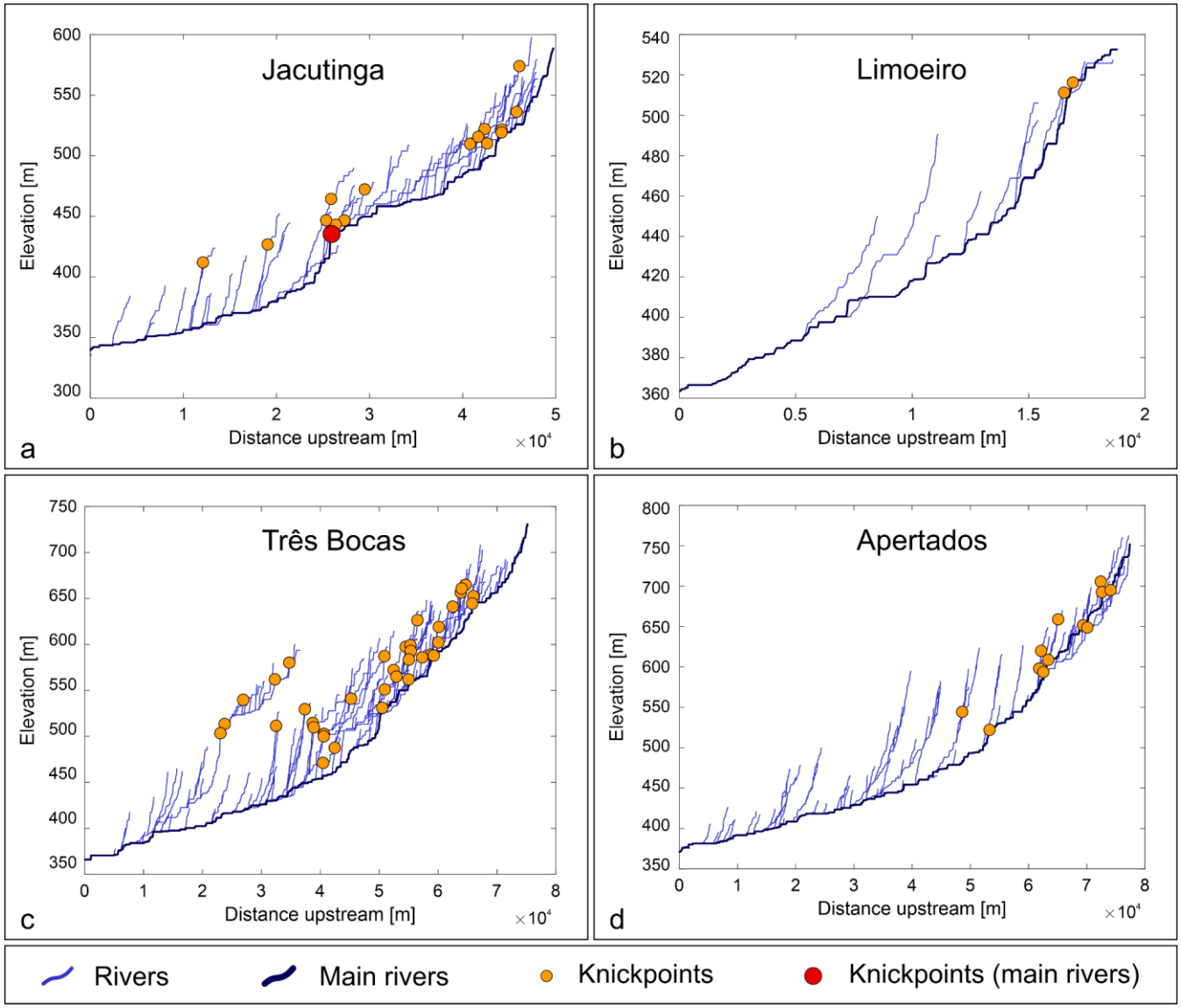

Figure 9. Longitudinal profiles of the main rivers in the study area and associated knickpoints.

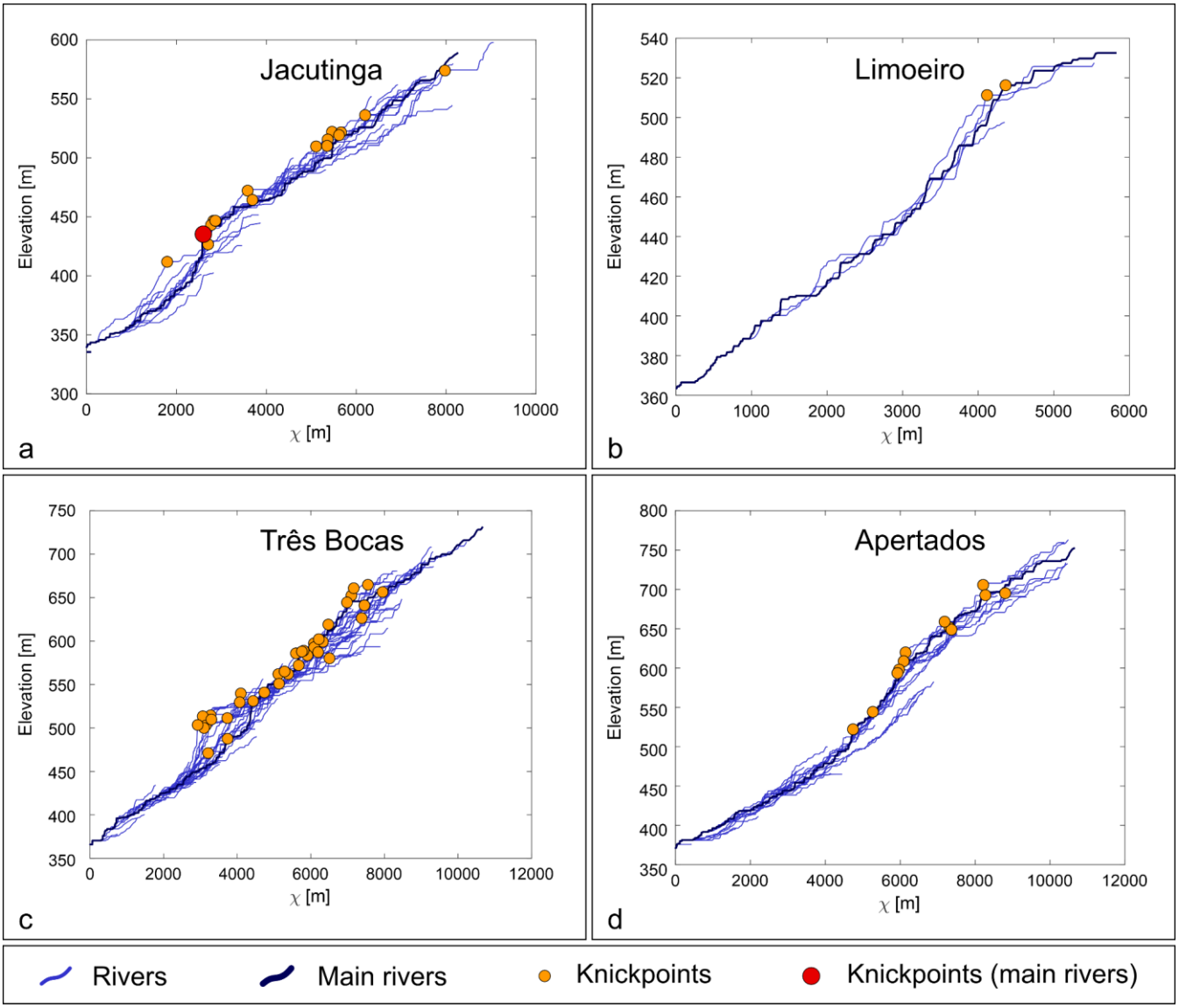

Figure 10. Chi-plots and associated knickpoints of the main analyzed hydrographic basins.

4.4. Structural analysis of field data

From the field survey, 203 fault plane attitudes were obtained (Figure 11), of which 98% were determined as strike-slip faults and 2% as normal faults. East-West trending faults predominate, ranging between ENE-WSW and WNW-ESE directions, followed by NNE-SSW, NW-SE, and NE-SW faults. In the planes of 90 strike-slip faults, it was possible to identify kinematic indicators, with predominantly horizontal to sub-horizontal dips.

The faults were described as continuous, rectilinear to curvilinear structures, sometimes exhibiting cataclasis associated with damage zones with thicknesses between 0.2 and 1.0 meters (Figure 12). The fault planes are smooth to rough, and may be filled with minerals such as oxides, calcite, and clay minerals. Identified kinematic indicators include slickensides - mineral fiber streaks - conjugate fractures, crescent fractures, spoon fractures, and grooves (Figure 13).

The faults were separated into six families based on their directions: F1 (N71-90E), F2 (N41-70E), F3 (N16-40E), F4 (N15E-N15W), F5 (N16-40W), and F6 (N41-70W). This division allowed for a more accurate structural analysis of each fault family and facilitated subsequent systematization for determining paleostress directions in the WinTensor software.

Statistical predominance was observed in the strike-slip faults of the F1 family, with an equal number of sinistral and dextral movements, indicating tectonic reactivations in this direction. The F2 fault family, predominantly characterized by sinistral movements, showed a higher incidence of structures with ambiguous kinematics. In this context, occurrences of both dextral and sinistral movements on the same fault were observed,

suggesting reactivations of these structures. For families F3 and F4, dextral strike-slip faults predominated; unlike families F5 and F6, which were predominantly sinistral. Normal and transtensional faults also belong to the same systems as families F5 and F6, indicating structural directions where relief occurred.

The mean axes of the paleostress fields were defined at five field points (Figure 14), based on the systematization and analysis of fault data and kinematic information in the WinTensor software, which uses the method of right dihedra for its calculation routine. Kinematic and dynamic analyses allowed the interpretation of three paleostress fields in the region's rocks, with σ1 directions: (a) N25E-S205W, (b) N20W-S160E, and (c) a variable paleostress field between N75E-S255W and N75W-S105E. The shear relationships described in the field allowed us to verify that the E-W and NW-SE trending faults would be younger structures than those of the NE-SW direction, which are intersected and displaced by those faults.

The action of the N25E paleostress field would be responsible for the dextral kinematics of the F4 fault family and the sinistral kinematics of the F3 faults. The position of a N20W paleostress axis would be related to the dextral movement of F5 and the sinistral movement of F3 and F4. Finally, the N75E paleostress direction would be related to the dextral kinematics of the F2 fault family and the sinistral kinematics of the F1 and F5 fault families.

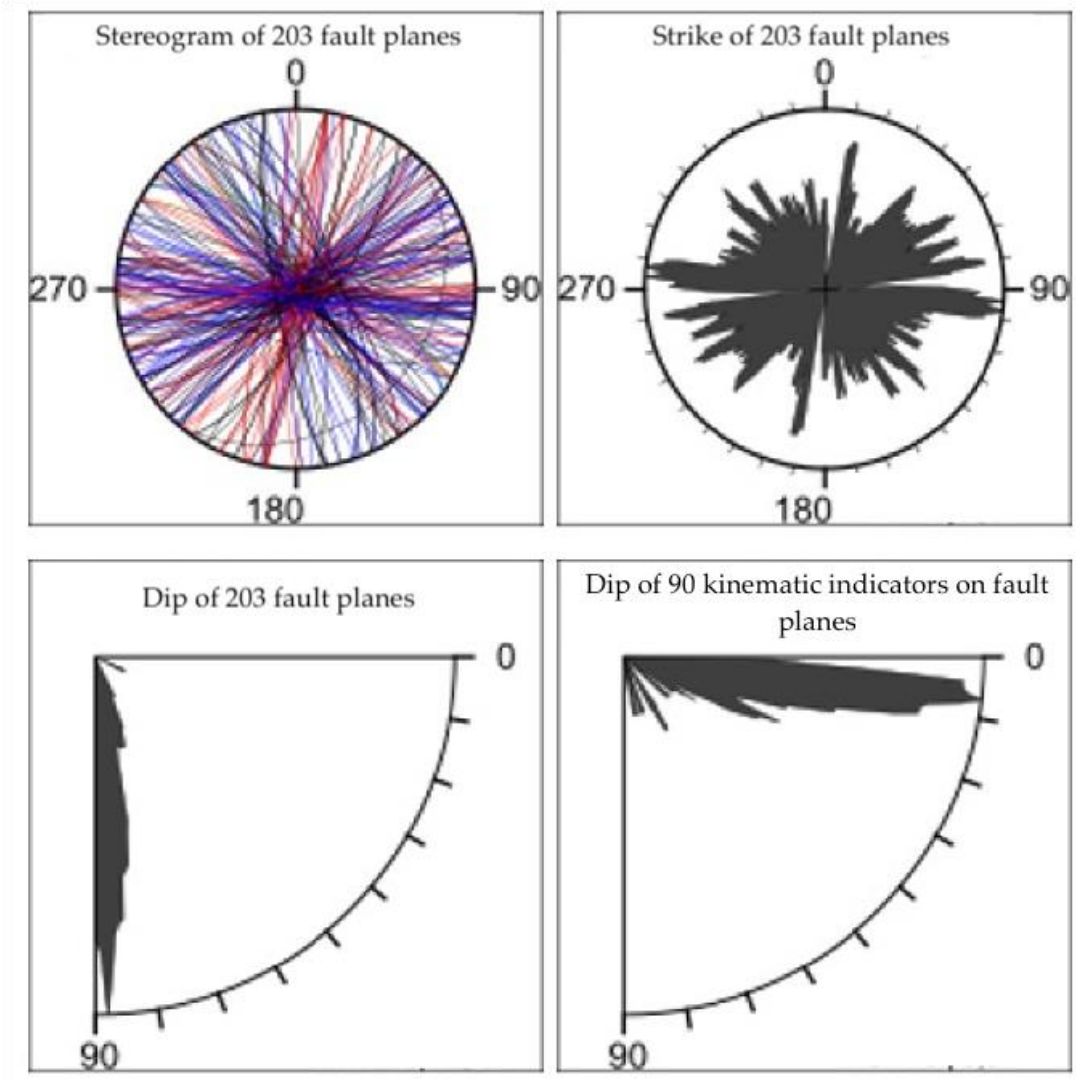

Figure 11. Stereograms illustrating the azimuthal distribution of the 203 fault planes measured during the fieldwork stage. Also illustrated are the dips of the planes and the kinematic indicators, recording almost all transcurrent faults in the study area.

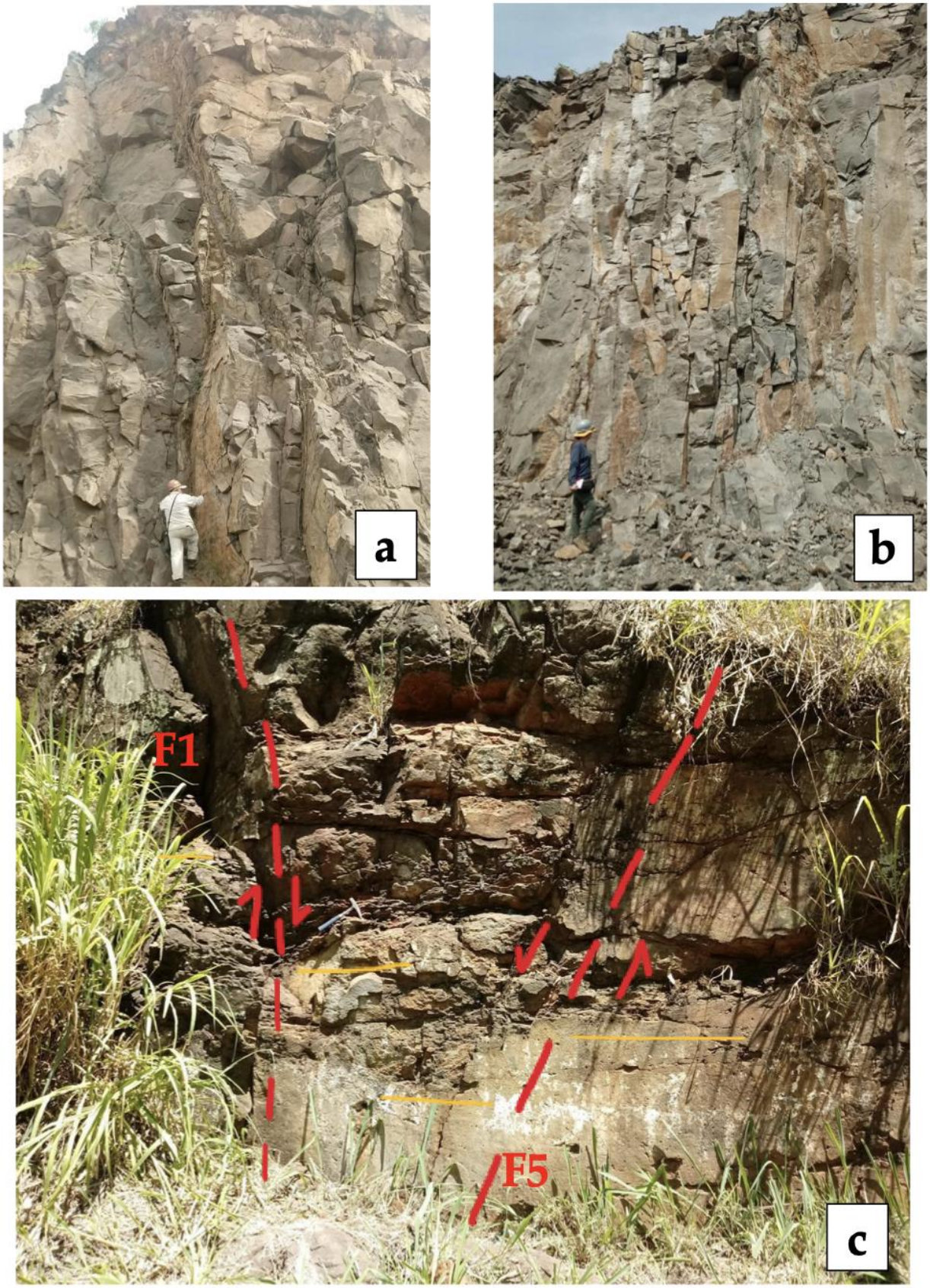

Figure 12. (a) Conjugate faults, forming a significant curviplanar fault plane with a wealth of kinematic indicators; (b) Pervasive and systematic faults, trending N75E, dextral; (c) Negative flower structure, formed by N35W/70NE faults (F5 family) and N82W/89NE faults (F1 family).

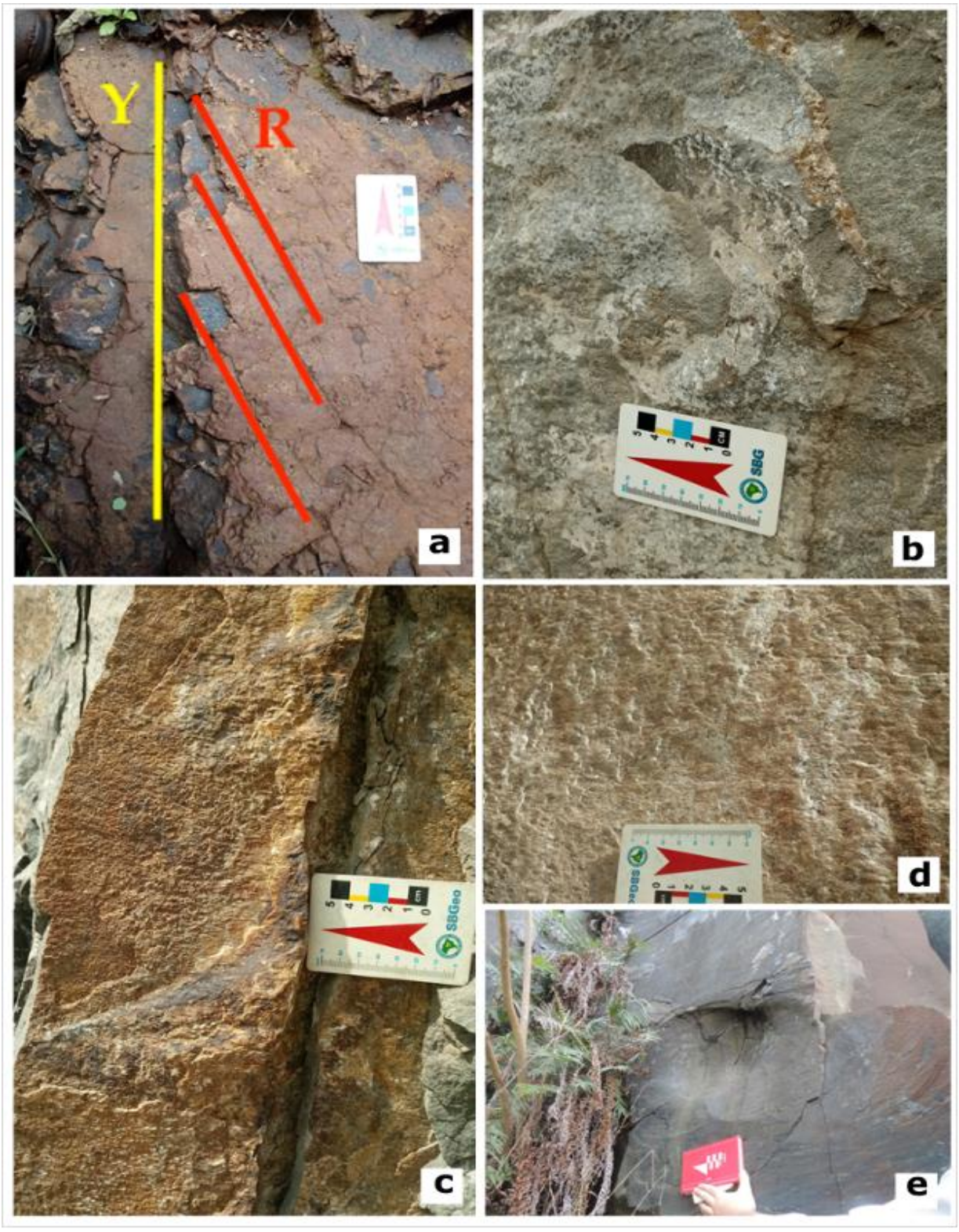

Figure 13. Kinematic indicators: (a) R parameter, where R fractures, synthetic, exhibit low angularity with the main fault (Y), forming so-called incongruent steps, or false steps; (b) and (e) spoon structure, kinematic indicators produced by the gouge material dragged along the fault plane during movement; (c) and (d) Combination of mineral slickensides and steps, produced by mineral crystallization and growth during movement along the fault plane. The arrows on the scale indicate the direction of movement of the missing block.

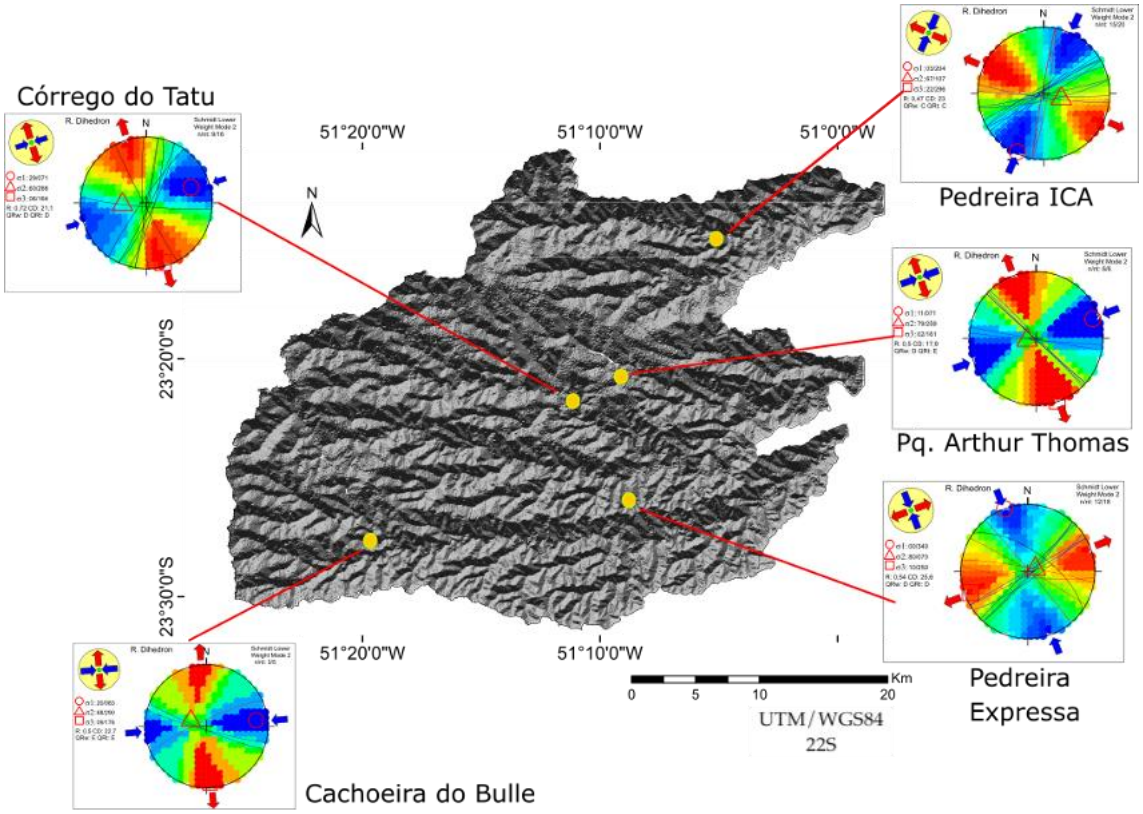

Figure 14. Paleostress directions determined by the method of right dihedrals at five field points in the study area.

5. Discussion

5.1. Dynamics of geomorphic processes

The geomorphic analysis of the topography and rivers indicates a landscape in a stage of adjustment to disturbances, likely of regional and local scale and occurring at different periods in the Cenozoic evolutionary history. The results suggest an erosive pattern of the topography driven by at least two pulses of regional uplift/base level fall, evidenced by clusters of knickpoints in chi-transformed profiles indicating an increase in *ksn* downstream (KIRBY; WHIPPLE, 2012); an older one, whose migrating incision wave currently shows around 700 m elevation, already reaching the headwaters near the regional divide of the Tibagi, Pirapó (to the west), and Ribeirão Vermelho (to the northwest) basins; a more recent wave, currently around 500 to 550 m elevation, and which shows interference from knickpoints generated at the upstream edge of the N50-60E escarpment, evidenced by the dispersion of channel slope ruptures, especially in the Três Bocas basin (Figs. 2; 10c). Visual analysis of the *chi x* elevation profiles allows estimating the magnitude of this more recent uplift/base level fall to be in the range of 100 to 150 m. This magnitude is consistent with factors such as denudational or flexural isostasy or far-field stress in the intraplate context of the southern-southeastern region of Brazil (c.f. CAMPOS et al., 2023).

The topographic asymmetry in the E-W direction, marked by narrow and elongated remnants of high plateaus to the west (>800 m) contrasting with the more dissected portion near the Tibagi valley floor (between 400 and 500 m), appears disturbed by a N50-60E band delineated by steeper slope and *ksn* values, in addition to aligned and migrating knickpoints from its northwest edge (Fig. 2). Along the band and downstream of it, the E-W channels tend to inflect and assume the same NE direction, indicating control by this N50-60E structure. This geomorphic configuration associated spatially with greater heights of knickpoints and concentration of recent seismic epicenters (Figs. 1 and 2) suggests probable reactivation of this N50-60E structure, where knickpoints of different elevations are aligned and propagate upstream from the escarpment, signaling the sector of highest uplift rate (BOULTON et al., 2014; CAMPOS et al., 2023), contrasting with the downstream sector of the escarpment with lower channels and increments in sinuosity. In this sense, the high block of the escarpment to the west and northwest explains the occurrence of straight channels, entrenched in fractures and faults of the basaltic basement. It is noteworthy that as one approaches the intersection between the N50-60E fault scarp and the São Jerônimo-Curiúva ~N20W lineament

in the southwest portion of the area, the total incision in the main E-W basins increases, reaching ~300 m. Additionally, there is a change in the migration direction of the divide from north to south, promoting an increase in the area of the Apertados river basin (Fig. 6) and, consequently, an acceleration in erosion rate in this area and progressively captures of adjacent basin headwaters. Thus, our results reveal differentiated uplift/base level fall among the E-W basins, main tributaries of the left bank of the Tibagi River in the study area, with an increase in uplift/base level fall to the south as one approaches the São Jerônimo-Curiúva Lineament. The inversion of the migration direction of the divide between the basins suggests that those cut by the São Jerônimo-Curiúva Lineament (Apertados and Três Bocas) are more influenced by it than by the Paranapanema Lineament of ~E-W direction immediately north of the area.

The analysis of the drainage basin symmetry reveals asymmetries in the main channels, indicating tectonic block tilting processes and possible block rotation, consistent with the analysis of divide migration. The Três Bocas and Apertados basins showed higher values of the asymmetry factor (AF), followed by Limoeiro, Jacutinga, Cafezal, and Cambé, demonstrating that, comparatively, the migration of the channel towards the basin edge was uneven. On the other hand, the analysis of the transverse topography symmetry factor (T) shows preferentially tilted areas in each basin, with greater asymmetries in the upper and middle reaches, decreasing as one approaches the channel mouths. This basin symmetry configuration denotes a stepped block geometry, with three blocks delimited by WNW-ESE (and ENE-WSW) lineaments. These lineaments correspond to strike-slip faults that, associated with normal movement components, enable a transtensive arrangement, responsible for block rotation and the tilting of the central block southward, disagreeing with the regional relief slope.

5.2. Cenozoic tectonics and its relationship with landscape dynamics

The results of paleostress analyses, obtained from the kinematic analysis of field rupture data, revealed the main average stress field directions ($\sigma 1$): N30E, N20W, and N75E. These paleostress directions correspond to different proposed tectonic pulses, as a single deformational event could not generate the spatial arrangement of structures with the heterogeneous kinematics of faults observed in the area.

The N50-60E escarpment structure is associated with the Guaxupé Fault, an important Proterozoic shear zone marked by recurrent tectonic reactivations during the formation and deformation of the Paraná Basin, from the Paleozoic to the Cenozoic. The N50-60E structure exhibits predominantly sinistral strike-slip fault planes. The direction and kinematics of this set of faults indicate that they are older than the faults-oriented NW-SE and E-W. These observations are supported by several recent studies conducted in the south and southeast of Brazil (PEYERL et al., 2018; PINHEIRO et al., 2019; PINHEIRO; CIANFARRA, 2021; SILVA et al., 2021; FARIAS et al., 2022; GIMENEZ et al., 2022; SANTOS et al., 2022). We consider the N30E paleostress axis responsible for generating dextral strike-slip faults with N-S orientation and reactivating sinistral faults with N40-60E orientation. In the field, these structures are better represented in outcrops to the north of the area, near the mouth of the Lindoia river into the Jacutinga river (Figure 15 - c, d). This tectonic pulse would have been responsible for the reactivation of NE-SW faults, such as the Guaxupé Fault and subsidiary structures, which culminated in the initiation of the N50-60E escarpment formation. Along the Jacutinga river, the altimetric breaks were directly related to the structuring of N-S oriented faults, combined with NE-SW trending faults.

The N40-55W oriented lineaments correspond regionally to the Ponta Grossa Arch and locally to the São Jerônimo-Curiúva Lineament. They control the drainage network and dissect the N50-60E escarpment. The Cambé river basin, the most seismogenic among those evaluated (Figure 1), is nestled in a valley with N55W orientation, differing from the others with orientations close to E-W. There is also an epicenter near the headwaters of the Limoeiro river with an ~E-W direction and adjacent to the Cambé river basin. The common factor for the epicenters of both basins is the N50-60E structure and aligned knickpoints in that direction, not the general orientation of the basins. Thus, our results indicate a strong relationship between recent seismic epicenters and knickpoints aligned along the N50-60E escarpment, including those with greater height in the area (Figs. 2, 3, and 5). These results corroborate the previous study by Santos et al. (2022), which points to a preferential spatial association of Guaxupé Fault segment reactivation in sectors where it intersects with the São Jerônimo-Curiúva Lineament. In the field, NW-SE oriented faults were predominantly described as sinistral strike-slip faults, although dextral ones also occur, in addition to few normal faults.

The N20W paleostress axis was better observed in the southeast of the area, in the lower course of the Três Bocas river basin, near the boundary with the Apertados basin. This stress direction is related to the nucleation of

dextral strike-slip faults with N40-55W orientation, structures linked to the Ponta Grossa Arch, such as the São Jerônimo-Curiúva Lineament and the NW-SE faults parallel to it (Figure 15A, B). It is a NNW-SSE compressive pulse responsible, also, for reactivations in the NW-SE structuring of the basement, which allowed the dissection of the pre-existing NE-SW oriented escarpment.

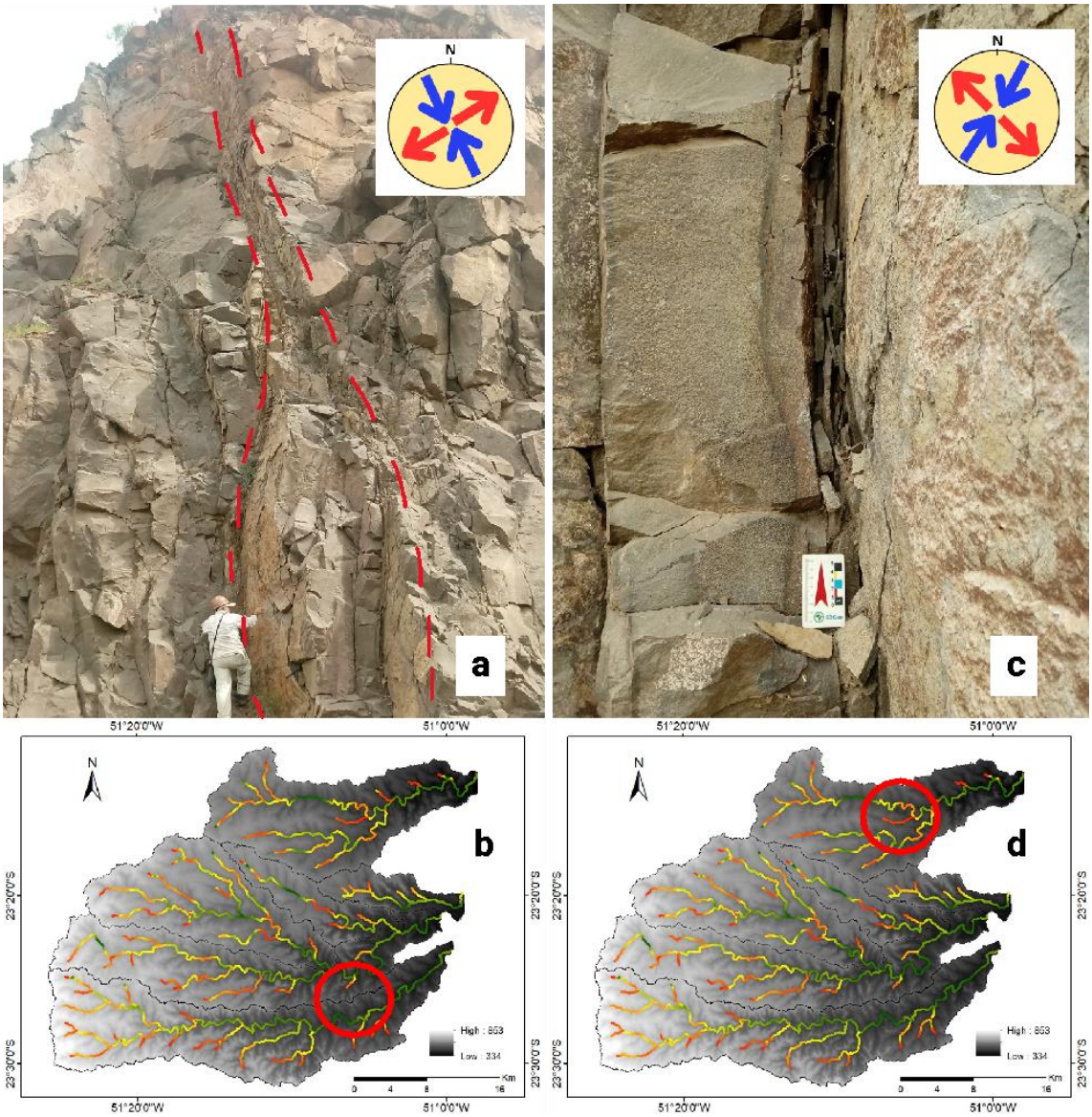

Figure 15. Outcrop at Expressa quarry (a), in the Três Bocas River basin (red circle in image b)): conjugate strike-slip faults with N35-55W orientation, parallel to the São Jerônimo-Curiúva lineament, whose dextral activation is associated with compressive paleostress N20W. ICA Quarry (c), Jacutinga River basin (red circle in image d)): mapped dextral N-S and sinistral N40-60E strike-slip faults: activations would be linked to the paleostress tensor N30E.

The strike-slip faults with a normal component and the purely normal faults concentrated in the N25-35W and N55-65W directions, configuring negative flower structures (Figure 12C). Their presence in the study area allows defining a transtensive structural arrangement.

The lineaments in the E-W direction (ENE-WSW, ESE-WNW) correspond to the direction of the Paranapanema Lineament and the São Sebastião Lineament (SOARES, 1991). The faults in this direction are represented by the valleys and interfluves of the main analyzed channels, showing a marked parallelism. Field surveys showed that faults in the E-W direction were the most statistically representative, corresponding to both sinistral and dextral strike-slip faults.

The paleostress direction with an azimuth of N75E was well characterized in the central block, in the Cambé and Cafezal basins (Figure 16), and in the southern block, in the Apertados River basin (Figure 17). It is related to the dextral reactivations of NE-SW strike-slip faults and sinistral reactivations in NW-SE faults. The E-W faults, when subjected to this paleostress direction, would have responded through variations in the activation of the dextral-sinistral binary. This pulse would be responsible for the escarpments along strike-slip faults with an approximately E-W direction, which delimit much of the analyzed basins and tectonically tilted blocks. Spatial arrangements between efforts and pre-existing structures may have been responsible for the transtensive situations that culminated in rotations and tilting along this direction.

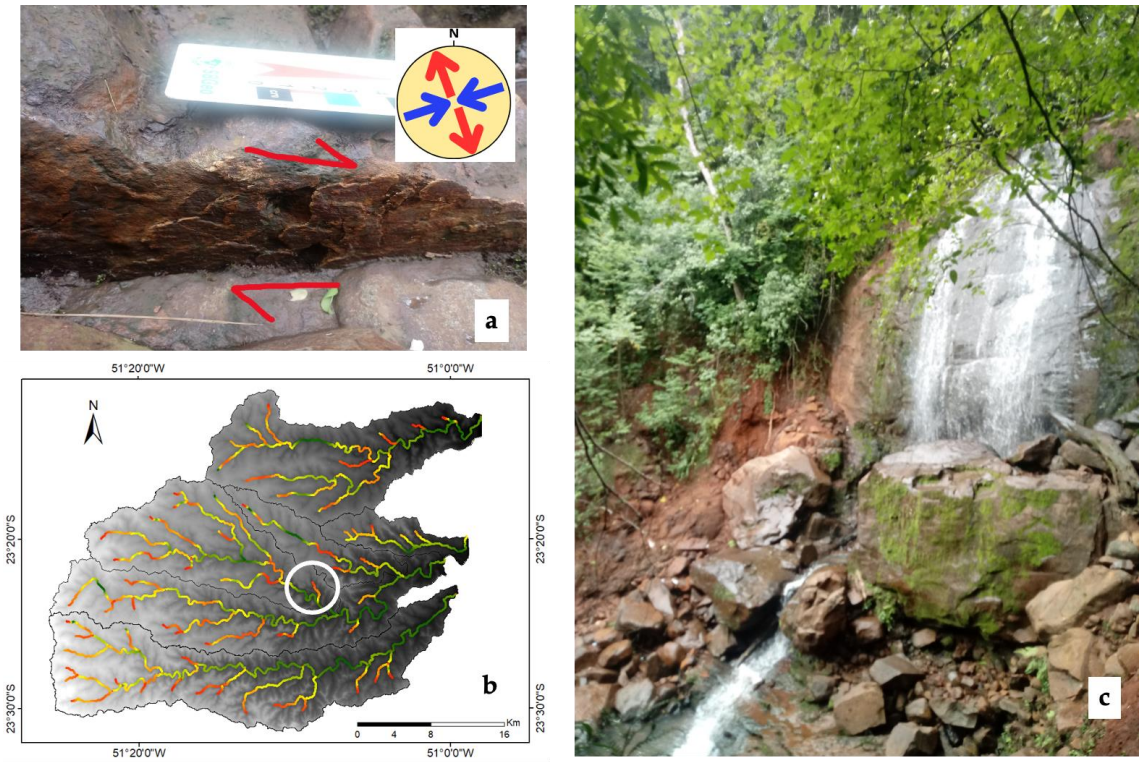

Figure 16. Cachoeira do Tatu (c), located in the Cafezal River basin (white circle in figure b), represents a significant knickpoint conditioned by a dextral strike-slip fault zone with a N10E direction (a). Channel ruptures generated by N-S trending faults were mapped in the central block (Cambé and Cafezal basins), being responsible for escarpments in drainage channels entrenched in E-W trending faults, and they are associated with the paleostress axis N75E (a).

The N-S fault trend (NNW-SSE, NNE-SSW), although less represented in the lineament directions, controls the rearrangement of the drainage network in the analyzed basins, conditioning parallelisms, sharp inflections, and channel captures associated with knickpoints. The tectonic control exerted by the N-S trending faults could be observed in the Córrego do Tatu (Figure 16), a tributary of the Cafezal River, where a significant knickpoint occurs conditioned by a dextral strike-slip fault zone with a N10E direction.

The exact chronological hierarchy among the compressive pulses is hindered by the absence of field data, such as faulted colluvium or absolute dating. However, establishing a relative chronology of the events can be inferred from correlations with previous studies that addressed and/or dated post-Cretaceous brittle deformation events in southern and southeastern Brazil.

The compressive pulse N30E was the first among the identified events in the researched area and would have occurred from the Neocretaceous to the Paleogene, with the action of a compressive paleostress (σ1) with a N30E direction. The compressive event in this direction was described by Strugale et al. (2007) in the Ponta Grossa Arch region and Jacques et al. (2014) on the eastern edge of the Paraná Basin (SC), occurring between the Neocretaceous and the Paleogene. Riccomini (1995), in the Cananeia Massif (SP), verified the action of a σ1 NE-SW paleostress during the Paleogene (Eocene), associated with the initial tectonics forming the rift basins of the RCSB. More recently, Peyerl et al. (2018) and Santos et al. (2019), respectively, in the basaltic plateau of the PIP in the Guarapuava (PR) and Chapecó (SC) regions, also consider such a maximum compression event NE-SW in the Paleogene.

However, studies conducted in the Cinzas River basin, adjacent to the Tibagi River basin, suggest a probable Miocene age for such a stress regime in the region (c.f. SANTOS et al., 2022).

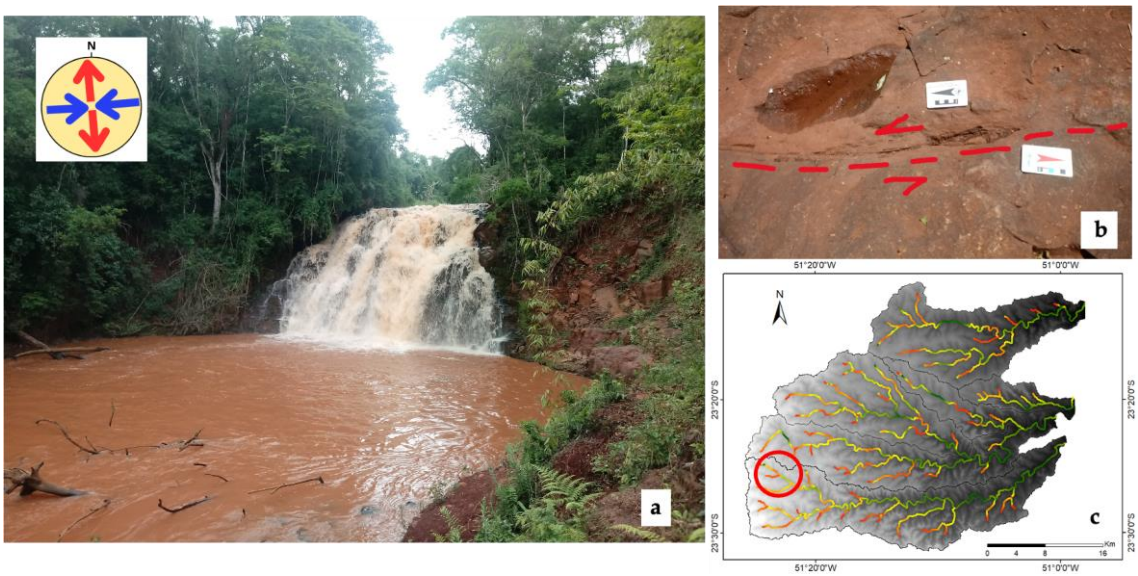

Figure 17. Cachoeira do Bulle (a), located in the Apertados River basin (red circle in image c)): sinistral strike-slip faults (b) with a N55W direction were mapped at the site, parallel to the São Jerônimo-Curiúva lineament, into which this stretch of the river fits. These structures are associated with compressive paleostress of approximately N75E direction, which would also be responsible for the escarpments along strike-slip faults of approximately E-W direction, such as the fault generating the knickpoint at this location.

The activation of this compressive axis would have been responsible for the sinistral reactivation of strike-slip faults with N40-70E direction, corresponding to the important pre-Cambrian structuring of the Paraná Basin, as well as for the dextral activation of N-S strike-slip faults. This deformational pulse could have reactivated during this period the fault segment with N50-60E direction present in the area, associated with the Guaxupé Fault, constituting a strike-slip weakness zone. Our results point to a subsequent reactivation of this structure, since the drainage signatures observed would have disappeared from the landscape if they were related to the Paleogene, considering the time scale of fluvial responses to disturbances of 1–5 Ma (WHITTAKER; BOULTON, 2012), and even, if it could be extended due to homogeneous substrates with very resistant lithologies, which is not the case of the Tibagi basin, such an extension of time would not date back to the Paleogene.

Subsequently, there would have been a second compressive pulse in the Plio-Pleistocene, related to the activation of compressive paleostress (σ1) with N20W direction. This paleostress would have been responsible for the dextral activation of NW-SE strike-slip faults, equivalent to the faults of the Ponta Grossa Arch, as well as for the sinistral activation of WNW-ESE strike-slip faults. This paleostress direction is associated with the compressive paleotensor (σ1) verified in the Curitiba Basin (CHAVEZ-KUZ; SALAMUNI, 2008), and in other regions of the basaltic plateau and southeastern Brazil (PEYERL et al., 2018; SANTOS et al., 2019a; PINHEIRO et al., 2019; PINHEIRO; CIANFARRA, 2021; SILVA et al., 2021; CIANFARRA et al., 2022), responsible for sinistrally activating the N-S transcurrent faults and dextrally activating the NW-SE transcurrent faults.

Finally, there would be a tectonic pulse related to compressive paleostress in the approximate direction of N75E, responsible for activating the dextral-sinistral binary in the WNW-ESE and ENE-WSW strike-slip faults and conditioning scarps and drainage segments such as those of the Cambé River and the channel migrations of local hydrographic basins. This paleostress direction was verified by Riccomini (1995), Salvador and Riccomini (1995), Salamuni (1998), Salamuni et al. (2004), and Santos et al. (2022) and characterized as active between the Pleistocene and Holocene. It was also verified in the works of Peyerl et al. (2018) and Santos et al. (2019a) in the rocks of the PIP. According to Assumpção et al. (2016), this paleostress direction corresponds to the current stress field to which the Brazilian platform is subject, due to the interaction of forces between the South American and Nazca plates, varying near the E-W axis. Thus, since the Pleistocene, a compressive stress (σ1) would have been acting in the N75E direction, associated with far-field stress acting on the Brazilian platform due to the interaction with forces

resulting from the movements of the South American and Nazca plates. The activation of this compressive axis would be associated with the movement of the strike-slip faults with a direction close to E-W, in a sinistral manner. These faults condition most of the edges of the analyzed hydrographic basins, and a marked parallelism in drainage in this direction.

The results suggest a relationship between seismic epicenters and segments of the N50-60E fault. The presence of knickpoints aligned along the fault and migrating towards the block with higher uplift rates upstream of the escarpment indicates reactivation prior to this more recent seismic activity, thus characterizing recurrent reactivation over time. The age of such reactivation is still uncertain, but the signatures of longitudinal river profiles allow us to rule out a relationship with the Paleogene tectonic pulse. The location of recorded seismic epicenters generally coincides in the field with the regions of intersection of the N50-60E fault, which conditions slope ruptures in the escarpment zone, and the lineaments of N40-55W direction, equivalent to the São Jerônimo-Curiúva lineament and the Ponta Grossa Arch. Such observations corroborate a previous study by Santos et al. (2022), which identifies sectors of intersection between the Guaxupé Fault and the São Jerônimo-Curiúva Lineament as preferential zones of Neogene/Quaternary reactivation. It is not uncommon to observe in the field the filling and growth of minerals, especially calcite and manganese, along fault planes, which can aid in determining the age of recurrent reactivation pulses of such faults through the dating of these minerals in future studies (cf. CALEGARI et al., 2020).

Our results, based on the combination of geological field data, structural analysis, and geomorphic analysis, allow the elaboration of a morphotectonic model of the Londrina region (Figure 18).

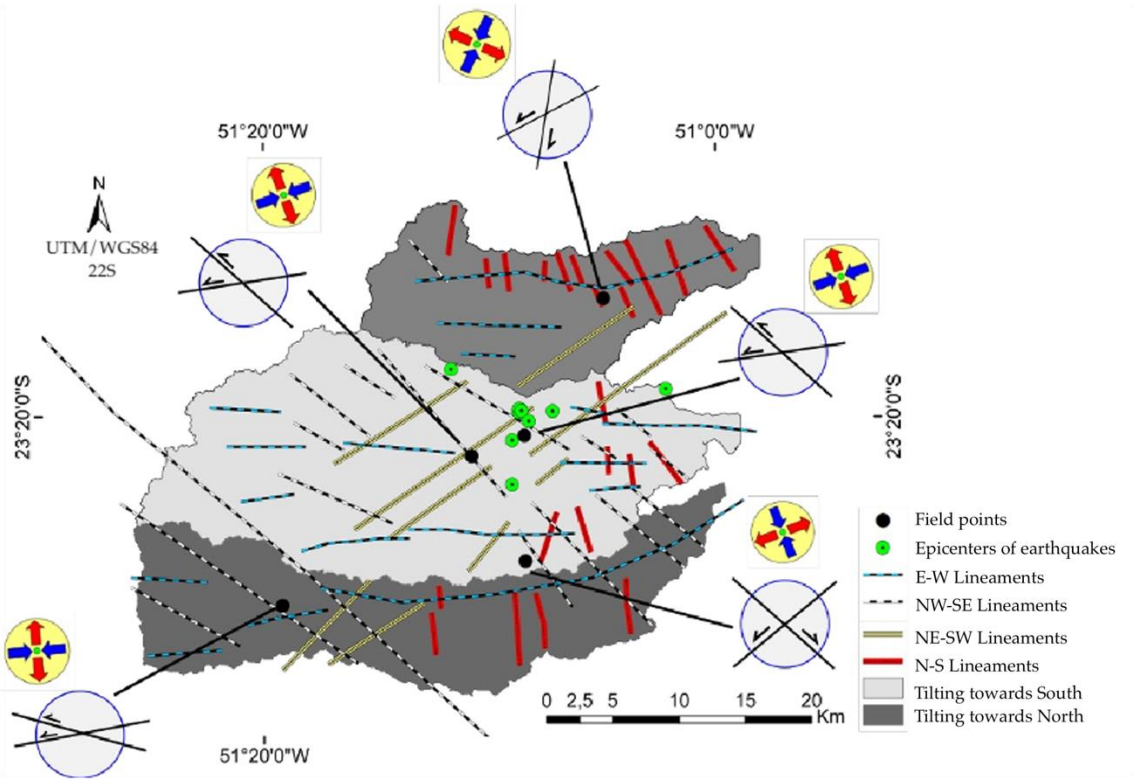

Figure 18. Proposed morphotectonic model for the study area, showing the locations of registered seismic epicenters, the outline of relief lineaments, and indications of block tilting. For each field point, there is a representation of the paleostress axes (blue arrows correspond to the maximum compression axis σ1) and a schematic representation of the arrangement of the main fault families observed at the point, including their kinematics.

The model proposes an arrangement with northern, central, and southern blocks, tilted in different directions, bounded by strike-slip faults associated with transpressive movements (Figure 18). These processes complement the possibility of subsidence related to transpression at the boundaries between the blocks, under the NW-SE and WNW-ESE directions. Variations in the asymmetry factors of the analyzed basins indicated different tilting directions, associated with responses to tectonic stresses. The results suggest that the substrate exhibits a geometry

in structural domains bounded by faults that tilt in different directions, in a transpressive arrangement involving differentiated block rotation along reactivated substrate faults (Figure 18).

6. Conclusions

In this study, we explored the relationships between surface processes and tectonics, analyzing signals in the topography, rivers, and basaltic rocks of the substrate, aiming for a deeper understanding of recent seismicity in the area. Geomorphic and structural analyses allowed us to verify the influence of post-Cretaceous tectonic control on the landscape dynamics of the Londrina region. Our findings point to external factors triggering recurrent disturbances at both regional and local scales, implying a state of landscape transience towards an adjustment, not yet achieved, to new conditions.

The results reveal two pulses of uplift/base level fall recorded by the drainage network. Reactivations of segments, especially along the intersection sectors of important pre-existing structures, seem to interfere with this dynamic, likely generating differentiation in uplift rates between basins, gain and loss of area in these basins, and block rotation under a transtensive regime.

From the perspective of the tectonic process that has affected the landscape since at least the beginning of the Paleogene, we identified three deformational pulses: (a) N30E paleostress axis responsible for generating dextral strike-slip faults of N-S direction and reactivation of sinistral faults of N40-60E direction. This pulse would have been responsible for reactivations in NE-SW faults, such as the Guaxupé fault and subsidiary structures, which could have triggered the onset of the N50-60E escarpment formation; (b) N20W paleostress axis related to the activation of structures linked to the Ponta Grossa Arch, such as the N40-55W strike-slip faults reactivated with dextral kinematics, such as the São Jerônimo-Curiúva lineament; (c) N75E paleostress axis related to the reactivation of N40-70E faults with dextral kinematics and reactivation of N70E to E-W and N15-40W faults with sinistral kinematics.

The earthquakes recorded in recent years are directly related to reactivation along an N50-60E fault scarp, whose geomorphic and kinematic signatures indicate recurrence of tectonic movement over time.

The conclusions of this article broaden the knowledge of intraplate tectonics between the Neocretaceous/Paleogene and the Pleistocene and emphasize the complexity, challenge, and need for a deeper understanding of landscape evolution within plates, especially the South American Plate. In this regard, it is expected that future studies can advance in determining the age of recurrent reactivation pulses of such faults through dating of grown and stretched filling minerals (such as calcite, illite, and manganese) along some of their segments.

Author contributions: A.C.B.S.: conception, methodology, software, validation, formal analysis, investigation, resources, data curation, writing—original draft preparation, writing—review and editing, and funding acquisition; E.S.: conception, methodology, validation, formal analysis, investigation, resources, data curation, writing—original draft preparation, writing—review and editing, supervision and funding acquisition; M.S.: methodology, software, validation, formal analysis, data curation, writing—original draft preparation, writing—review and editing and supervision; S.S.C.: methodology, software, validation, formal analysis, data curation, and writing—review and editing. All authors have read and agreed to the published version of the manuscript.

Financing: This research was funded by the Coordination for the Improvement of Higher Education Personnel (CAPES) through a financial aid grant that supported the author in project expenses (Code 001), and by the National Council for Scientific and Technological Development (CNPq) through Productivity in Research grants (Process 307738/2019-1) awarded to co-author E. Salamuni.

Acknowledgements: The authors thank the Neotectonics group of the Federal University of Paraná (UFPR - Curitiba, Brazil), as well as the Graduate Program in Geology at UFPR. Scientific results were obtained using Win-Tensor, a software developed by Dr. Damien Delvaux of the Royal Museum for Central Africa in Tervuren, Belgium, and we appreciate his availability.

Conflict of Interest: The authors declare no conflict of interest.

References

1. AGURTO-DETZEL; H., ASSUMPÇÃO; M. BIANCHI, M.; PIRCHINER, M. Intraplate seismicity in mid-plate South America: correlations with geophysical lithospheric parameters. In: LANDGRAF, A., KÜBLER, S., HINTERSBERGER, E., STEIN, S. (Ed.). **Seismicity, Fault Rupture and Earthquake Hazards in Slowly Deforming Regions**. London: Geological Society Special Publications, 2017. p. 73-90.
2. ANGELIER, J.; MECHLER, P. Sur une méthode graphique de recherche des contraintes principales également utilisable en tectonique et en sismologie: la méthode des dièdres droits. **Bulletin de la Societé Géologique de France**, v. 19, n. 6, p. 1309-1318, 1977. DOI: 10.2113/gssgfbull.S7-XIX.6.1309
3. ASSUMPÇÃO, M.; DIAS, F.B.; ZEVALLOS, I.; NALIBOFF, J.B. Intraplate stress field in South America from earthquake focal mechanisms. **Journal of South American Earth Sciences**, v. 71, p. 278-295, 2016. DOI: 10.1016/j.sames.2016.07.005
4. BARCELOS, J.H. **Reconstrução paleogeográfica da sedimentação do Grupo Bauru baseada na sua redefinição estratigráfica parcial em território paulista e no estudo preliminar for a do estado de São Paulo**. Tese Livre-Doc – IGCE, Universidade Estadual Paulista, Rio Claro. 1984. 190 p.
5. BARTORELLI, A. Origem das grandes cachoeiras do planalto basáltico da Bacia do Paraná: evolução quaternária e geomorfologia. In: MANTESSO-NETO, V. (et al.). **Geologia do continente sul-americano: evolução da obra de Fernando Flávio Marques de Almeida**. São Paulo: Editora Beca, 2004. p. 95-111.
6. BEESON, H. B.; MCCOY S. W.; KEEN-ZEBERT, A. Geometric disequilibrium of river basins produces long-lived transient landscapes. **Earth And Planetary Science Letters**, v. 475, p. 34-43, 2017. DOI: 10.1016/j.epsl.2017.07.010
7. BELLIENI, G.; COMIN-CHIARAMONTI, P.; MARQUES, S. L.; MELFI, A. J.; NARDY, A. J. C.; PAPATRECHAS, C.; PICCIRILLO, E. M.; ROISENBERG, A.; STOLFA, D. Petrogenetic aspects of acid and basaltic lavas from the Paraná plateau (Brazil): geological, mineralogical, and petrochemical relationships. **Journal of Petrology**, v. 27, n. 4, p. 915-944, 1986. DOI: 10.1093/petrology/27.4.915
8. BISHOP, P. Drainage rearrangement by river capture, beheading and diversion. **Progress in Physical Geography: Earth and Environment**, v. 19, n. 4, 1995. DOI: 10.1177/030913339501900402
9. BOULTON, S. J.; STOKES, M.; MATHER, A. E. Transient fluvial incision as an indicator of active faulting and Plio-Quaternary uplift of the Moroccan High Atlas. **Tectonophysics**, v. 633, p. 16-33, 2014. DOI: 10.1016/j.tecto.2014.06.032
10. BULL, W. B. **Tectonically active landscapes.** Chichester: Wiley-Blackwell, 2007. 320 p.
11. BURBANK, D.W.; ANDERSON, R.A. **Tectonic Geomorphology**. 2ª Ed. Malden: Blackwell Science, 2011. 468 p.
12. CALEGARI, S. S.; AIOLFI, T. R.; NEVES, M. A.; SOARES, C. C. V.; MARQUES, R. A.; CAXITO, F. A. Filling Materials in Brittle Structures as Indicator of Cenozoic Tectonic Events in Southeastern Brazil. **Anuário do Instituto de Geociências**, v. 43, n. 2, p. 237-254, 2020. DOI: 10.11137/2020_2_237_254
13. CALEGARI, S. S.; PEIFER, D.; NEVES, M. A.; CAXITO, F.A. Post-Miocene topographic rejuvenation in an elevated passive continental margin not characterized by a sharp escarpment (northern end of the Mantiqueira Range, Brazil). **Geomorphology**, v. 393, n. 15, 2021. DOI: 10.1016/j.geomorph.2021.107946
14. CAMPOS, D. S.; SANTOS, M.; MARQUES, K. P. P.; SILVA, A. C.; TORRADO, P. V. Impact of tectonic topographic rejuvenation in landscapes with high bedrock/duricrust strength: Insights from geomorphic evidence in a post-rifted region (SE Brazil). **Geomorphology**, v. 435, 2023. DOI: 10.1016/j.geomorph.2023.108749
15. CHAVEZ-KUS, L.; SALAMUNI, E. Evidência de tensão N-S intraplaca no Neógeno - Complexo Atuba - região de Curitiba (PR). **Revista Brasileira de Geociências**, v.38, n.4, p.439-454, 2008. DOI: 10.25249/0375-7536.2008383439454
16. CIANFARRA, P.; PINHEIRO, M. R.; VILLELA, F. N. J.; SALVINI, F. Intraplate Strike-Slip Corridor within South America (NE Border of the Paraná Basin) Unveiled by Structural Analysis of Faults and Fracture Swarms. Geosciences, v. 12, v. 2, 2022. DOI: 10.3390/geosciences12020101
17. COX, R.T. Analysis of drainage-basin symmetry as a rapid technique to identify areas of possible Quaternary tilt block tectonics: as example from the Mississippi Embayment. **Geological Society of America Bulletin**, v.106, n.5, p.571-581, 1994. DOI: 10.1130/0016-7606
18. CREMON, É. H.; BETTIOL, G. M.; MAGNA JUNIOR, J. P.; MACEDO, F. C.; RABELO, M. W. O. Evaluation of altimetry from the COP-30 DEM in central-western Brazil. **Revista Brasileira de Cartografia**, v. 74, n. 3, p. 536–546, 2022. DOI: 10.14393/rbcv74n3-60846
19. DAVIS, W. M. **The Rivers and Valleys of Pennsylvania**. Kessinger Publishing, 1889. 76 p.
20. DELVAUX, D.; SPERNER, B. New aspects of tectonic stress inversion with reference to the TENSOR program. **Geological Society Special Publications,** v. 212, n. 1, p. 75–100, 2003. DOI: 10.1144/GSL.SP.2003.212.01.06
21. ESRI Inc. **ArcGIS Desktop: Release 10**. Environmental Systems Research Institute, Redlands, CA, 2016.
22. European Space Agency, Sinergise. **Copernicus Global Digital Elevation Model**. Distributed by Open Topography, 2021.

23. FARIAS, T.F.S; SALAMUNI, E.; PEYERL, W.R.L.; GIMENEZ, V.B. Post-Cretaceous brittle tectonics in the tunas Alkaline Complex, Paraná, Brazil. **Brazilian Journal Geology,** v. 52, n. 3, p. 1-24, 2022. DOI: 10.1590/2317-4889202220210041
24. FERNANDES, A. J.; AMARAL, G. Cenozoic tectonic events at the border of the Paraná Basin, São Paulo, Brazil. **Journal of South American Earth Sciences**, v. 14, n. 8, p. 911-931, 2002. DOI: 10.1016/S0895-9811(01)00078-5
25. FERREIRA, F.J.F. **Integração de dados aeromagnéticos e geológicos: configuração e evolução tectônica do Arco de Ponta Grossa.** Dissertação de Mestrado - Instituto de Geociências, Universidade de São Paulo, São Paulo. 1982. 170p.
26. FLINT, J. J. Stream gradient as a function of order, magnitude, and discharge. **Water Resources Research,** v. 10, n. 5, p. 969-973, 1974. DOI: 10.1029/WR010i005p00969
27. FORTE, A. M.; WHIPPLE, K. Short Communication: The Topographic Analysis Kit (TAK) for TopoToolbox. **Earth Surface Dynamics**, v: 7, n. 1, p: 87-95, 2019. DOI: 10.5194/esurf-7-87-2019
28. FRANCO-MAGALHÃES, A.O.; HACKSPACHER, P.C.; GLASMACHER, U.A.; SAAD, A.R. Rift to post-rift evolution of a "passive" continental margin: the Ponta Grossa Arch, SE Brazil. **International Journal of Earth Sciences,** v: 99, n. 7, p. 1599-1613, 2010. DOI: 10.1007/s00531-010-0556-8
29. FRANK, H. T.; GOMES, M.E.B.; FORMOSO, M.L.L. Rewiew of the areal extent and the volume of the Serra Geral Formation, Paraná Basin, South America. **Pesquisas em Geociências**, v. 36, n. 1, p. 49-57, 2009. DOI: 10.22456/1807-9806.17874
30. FURRIER, M.; SILVA, I. C. Geomorphology, morphometry and evidence of tectonics in the Araçaji Chart, Eastern Edge of Paraíba. **Revista Brasileira de Geografia Física**, v. 13, n. 4, p. 1570–1586, 2020. DOI: 10.26848/rbgf.v13.4.p1570-1586
31. FURRIER, M.; SILVA, I. C. Application of morphometric indices for the investigation of the structural and tectonic influences on the landform of the Atlantic-Type Continental Margin, Paraíba – Brazil. **Mercator**, v.20, e20014, p. 1-21, 2021. DOI: 10.4215/rm2021.e20014
32. GALLEN, S. F.; THIGPEN, J. R. Lithologic Controls on Focused Erosion, and Intraplate Earthquakes in the Eastern Tennessee Seismic Zone. **Geophysical Research Letters**, v. 45(18), p. 9569-9578, 2018.
33. GIMENEZ, V.B.; SALAMUNI, E.; SANTOS, J.M.S.; PEYERL, W.R.L.; FARIAS, T.F.S.; SANCHES, E. The role of fault reactivation in the geomorphological evolution of costal landforms on passive continents margins: evidence from a tectonic estuary in the southern Brazil. **Geomorphology**, v 402, p. 1-22, 2022. DOI: 10.1016/j.geomorph.2022.108132
34. GOMES, A.S.; LICHT, O.A.B.; VASCONCELLOS, E.M.G.; SOARES, J.S. Chemostratigraphy and evolution of the Paraná Igneous Province volcanism in the central portion of the state of Paraná, Southern Brazil. **Journal of Volcanology and Geothermal Research,** v. 355, p.253-269, 2018. DOI: 10.1016/j.jvolgeores.2017.09.002
35. GUTH, P. L.; GEOFFROY, T. M. LiDAR point cloud and ICESat-2 evaluation of 1 second global digital elevation models: Copernicus wins. **Transactions in GIS**, v. 25, n. 5, p. 2245-2261, 2021. DOI: 10.1111/tgis.12825
36. HACK, J.T. Interpretation of erosional topography in humid temperate regions. **American Journal of Science**, v. 258-A, p. 80-97, 1960.
37. HARE P.W.; GARDNER T.W. **Geomorphic indicators of vertical neotectonism along converging plate margins. Nicoya Peninsula, Costa Rica**. In*:* MORISAWA, M.; HACK, J.T. (Eds.) **Tectonic Geomorphology**: **Procedings 15th. Annual Binghamton Geomorphology Symposia.** 1985. p.76-104.
38. HARBOR, D.; BACASTOW, A.; HEATH, A.; ROGERS, J. Capturing variable knickpoint retreat in the Central Appalachians, USA. **Geografia Física e Dinâmica Quaternária**, v.28, n. 1, p.23-36, 2005.
39. HERGARTEN, S.; ROBL, J.; STUWE, K. Tectonic geomorphology at small catchment sizes extensions of the stream-power approach and the method. **Earth Surface Dynamics**, v. 3, n. 3, p. 689-714, 2015. DOI: 10.5194/esurfd-3-689-2015
40. HOWARD, A.D. Drainage analysis in geologic interpretation: a summation. **American Association of Petroleum Geologists Bulletin**, v.51, p.2246-2259. 1965. DOI: 10.1306/5D25C26D-16C1-11D7-8645000102C1865D
41. HOWARD, E. B.; KERBY, G. Channel changes in badlands. **Geological Society of America Bulletin**, v. 94, p. 739-752, 1983. DOI: 10.1130/0016-7606
42. JACQUES, P. D.; SALVADOR, E. D.; MACHADO, R.; GROHMANN, C. H.; NUMMER, A.R. Application of morphometry in neotectonic studies at the eastern edge of the Paraná Basin, Santa Catarina State, Brazil. **Geomorphology**, v: 213, p: 13-23, 2014. DOI: 10.1016/j.geomorph.2013.12.037
43. KELLER, E.A.; PINTER, N. **Active Tectonics: Earthquakes, Uplift, and Landscape**. Upper Saddle River: Prentice Hall, 2002. 432p.
44. KIRBY, E.; WHIPPLE, K. X. Expression of active tectonics in erosional landscapes. **Journal of Structural Geology**, v: 44, p: 54-75, 2012. DOI: 10.1016/j.jsg.2012.07.009
45. LICHT, O. A. B. A Revised Chemo-chrono-stratigraphy 4-D model for the extrusive rocks of Paraná Igneous Province. **Journal of Volcanology and Geothermal Research**, v. 355, p. 32-54, 2016. DOI: 10.1016/j.jvolgeores.2016.12.003

46. MILANI, J. M.; RAMOS, V. A. Orogenias paleozoicas no Domínio Sul-Ocidental do Gondwana e os ciclos de subsidência da Bacia do Paraná. **Revista Brasileira de Geociências**, v. 28, n. 4, p. 473-484, 1998. DOI: 10.25249/0375-7536.1998473484
47. MILANI, E. J.; MELO, J. H. G.; SOUZA, P.A.; FERNANDES, L.A.; FRANÇA, A.B. Bacia do Paraná. **Boletim de Geociências da Petrobras**: v.15, n.2, p.265-287, 2007.
48. MUDD, S. M.; CLUBB, F. J.; GAILLETON, B.; HURST, M. D. How concave are river channels? **Earth Surface Dynamics**, v. 6, p. 505-523, 2018. DOI: 10.5194/esurf-6-505-2018
49. NASCIMENTO, E.R.; SALAMUNI, E.; QUEIROZ, G.L.; HAUCK, P.A.; FIORI, A.P. Evidências de determinação morfotectônica e neotectônica no relevo da Serra do Mar no estado do Paraná. **Revista Brasileira de Geomorfologia:** v. 14, n. 13, p. 287-299, 2013. DOI: 10.20502/rbg.v14i3.402
50. PEIFER, D.; CREMON, É.H.; ALVES, F.C. Ferramentas modernas para a extração de métricas de gradientes fluviais a partir de MDES: uma revisão. **Revista Brasileira de Geomorfologia**, v. 21, n. 1, 2020. DOI: 10.20502/rbg.v21i1.1732
51. PEYERL, W. R. L.; SALAMUNI, E.; SANCHES, E.; NASCIMENTO, E. R.; SANTOS, J. M.; GIMENEZ, V. B.; SILVA, C. L.; FARIAS, T. F. Reativation of Taxaquara Fault and its morphotectonic influence on the evolution of Jordão River catchment, Paraná, Brasil. **Bras. Jour. of Geology**, v: 48, n. 3, 2018. DOI: 10.1590/2317-4889201820170110
52. PERRON, J.T.; ROYDEN, L. An integral approach to bedrock river profile analysis. **Earth Surface Processes Landforms,** v. 38, p. 570–576, 2013. DOI: 10.1002/esp.3302
53. PINHEIRO, M. R.; CIANFARRA, P.; VILLELA, F. N. J.; SALVINI, F. Tectonics of northeastern border of the Paraná Basin (Southeastern Brazil) revealed by lineament domain analysis. **Journal of South American Earth Sciences**, v. 94, 2019. DOI: 10.1016/j.jsames.2019.102231
54. PINHEIRO, M. R.; CIANFARRA, P. Brittle deformation in the Neoproterozoic basement of southeast Brazil: Traces of intraplate Cenozoic tectonics. **Geosciences**, v: 11, n. 7. 2021. DOI: 10.3390/geosciences11070270
55. PURINTON, B.; BOOKHAGEN, B. Beyond Vertical Point Accuracy: Assessing Inter-pixel Consistency in 30 m Global DEMs for the Arid Central Andes. **Frontiers in Earth Science**, v. 9, p.1-24, 2021. DOI:10.3389/feart.2021.758606.
56. QGIS Development Team. **QGIS Geographic Information System (versão 3.10)**. 2021. Disponível em: <http://qgis.osgeo.org>.
57. RICCOMINI, C. **O Rift Continental do Sudeste do Brasil.** Tese de Doutorado - Instituto de Geociências, Universidade de São Paulo, São Paulo. 1989. 256 p.
58. RICCOMINI, C. Padrão de fraturamento do maciço alcalino de Cananéia, estado de São Paulo: Relações com a tectônica Mesozoica-Cenozoica do sudeste do Brasil. **Revista Brasileira de Geociências,** v. 25, n. 2, p. 79-84, 1995. DOI: 10.25249/0375-7536.19957984
59. SALAMUNI, E. **Tectônica da Bacia Sedimentar de Curitiba (PR).** Tese de Doutorado - Instituto de Geociências e Ciências Exatas, Universidade Estadual Paulista, Rio Claro. 1998. 235 p.
60. SALAMUNI, E.; EBERT, H.D.; HASUI, Y. Morfotectônica da Bacia Sedimentar de Curitiba. **Revista Brasileira de Geociências**, v.34, n.4, p.469-478, 2004. DOI: 10.25249/0375-7536.2004344469478
61. SALVADOR, E.D.; RICCOMINI, C. Neotectônica da região do alto estrutural de Queluz (SP-RJ, Brasil). **Revista Brasileira de Geociências,** v. 25, n. 3, p. 151-164, 1995. DOI: 10.25249/0375-7536.1995151164
62. SANTOS, J. M.; SALAMUNI, E.; SILVA, C. L.; SANCHES, E.; GIMENEZ, V. B.; E. R., SANTOS. Morphotectonics in the Central-East Region of South Brazil: Implications for Catchments of the Lava-Tudo and Pelotas Rivers, State of Santa Catarina. **Geomorphology**, v. 328, p. 138-156, 2019. DOI: 10.1016/j.geomorph.2018.12.016
63. SANTOS, J. M.; SALAMUNI, E.; MORALES, N.; CASTRO, L. G.; SILVA, C. L.; SOUZA, I. A.; GIMENEZ, V. B.; OLIVEIRA, S. P. Aeromagnetic and structural characterization of dyke swarms in southeast Brazil: Evidence for Cenozoic reactivation of the Guapiara lineament, Ponta Grossa arch. **Journal of South American Earth Sciences,** v. 129, 2023. DOI: 10.1016/j.jsames.2023.104523
64. SANTOS, L. J. C.; OKA-FIORI, C.; CANALI, N. E.; FIORI, A. P.; SILVEIRA, C. T.; SILVA, J. M. F.; ROSS, J. L. C. Mapeamento geomorfológico do estado do Paraná. **Revista Brasileira de Geomorfologia**, v. 7, n. 2, 2006. DOI: 10.20502/rbg.v7i2.74
65. SANTOS, M. DOS; LADEIRA, F. S.B.; BATEZELLI, A. Indicadores geomórficos aplicados à investigação de deformação tectônica: uma revisão. **Revista Brasileira de Geomorfologia**. v. 20, n. 2, 2019b. DOI: 10.20502/rbg.v20i2.1564
66. SANTOS, M. DOS; LADEIRA, F. S.B.; BATEZELLI, A.; NUNES, J.O.R.; SALAMUNI, E.; SILVA, C.L. DA; MOLINA, E.C., MORAES, I.C. Interactions between tectonics, bedrock inheritance and geomorphic responses of rivers in a post-rifting upland (Ponta Grossa Arch region, Brazil). **Brazilian Journal Geology,** v. 52, n.1, p. 1-26, 2022. DOI: 10.1590/2317-4889202220210002
67. SCHUMM, S. A.; DUMONT, J. F.; HOLBROOK, J. M. **Active Tectonics and Alluvial Rivers**. Cambridge, United Kingdom: Cambridge University Press, 2000. 290 p.

68. SCHWANGHART, W.; SCHERLER, D. Bumps in river profiles: Uncertainty assessment and smoothing using quantile regression techniques. **Earth Surface Dynamics**, v. 5, n. 4, p. 821-839, 2017. DOI: 10.5194/esurf-5-821-2017
69. SILVA, B. A.; CALEGARI, M. R.; PINHEIRO, M. R.; FUJITA, R. H. Lithostructural and tectonic determinants in the geomorphic evolution of the basalt plateau – southern Brazil. **Journal of South American Earth Sciences,** v. 110, 2021. DOI: 10.1016/j.jsames.2021.103351
70. SILVA, I. C.; FURRIER, M. Análise morfológica e morfométrica das sub-bacias dos rios Cascata e Tinto, litoral norte do estado da Paraíba – Brasil. **Revista Brasileira de Geomorfologia**, v. 20, n. 2, 2019. DOI: 10.20502/rbg.v20i2.1505
71. SOARES A.P.; SOARES P.C.; BETTÚ D.F.; HOLZ, M. Compartimentação estrutural da Bacia do Paraná: a questão dos lineamentos e sua influência na distribuição do Sistema Aquífero Guarani. **Geociências UNESP**, v. 26, n.4, p. 297-311, 2007.
72. SOARES, P.C. **Tectônica sinsedimentar cíclica na Bacia do Paraná – controles**. Tese (Professor Titular) - Departamento de Geologia, Universidade Federal do Paraná, Curitiba. 1991. 131p.
73. STAIN, S.; MAZZOTTI, S. Continental Intraplate Earthquakes: Science, Hazard, and Policy Issues. **Geological Society of America,** v. 425, 402p, 2007. DOI: 10.1130/SPE425
74. STRUGALE, M.; ROSTIROLLA, S.P.; MANCINI, F.; PORTELA FILHO, C.V.; FERREIRA, F.J.F.; FREITAS R.C. Structural framework and Mesozoic-Cenozoic evolution of Ponta Grossa Arch, Paraná Basin, southern Brazil. **Journal of South American Earth Sciences**, v.24, p. 203-227, 2007. DOI: 10.1016/j.jsames.2007.05.003
75. The Mathworks Inc. **MATLAB (Version 18.3.0).** Natick, Massachusetts, USA, 2018.
76. THIEDE, D.S.; VASCONCELOS, P.M. Paraná flood basalts: Rapid extrusion hypothesis confirmed by new 40Ar/39Ar results. **Geology**, v. 38, n. 8, p. 747-750, 2010. DOI: 10.1130/G30919.1
77. WHIPPLE, K. X.; TUCKER, G. E. Dynamics of the stream-power river incision model: Implications for height limits of mountain ranges, landscape timescales, and research needs. **Journal Of Geophysical Research: Solid Earth**, v. 104 (B8), p. 17661-17674, 1999. DOI: 10.1029/1999JB900120
78. WHIPPLE, K. X.; TUCKER, G. E. Implications of sediment-flux-dependent river incision models for landscape evolution. **Journal Of Geophysical Research: Solid Earth**, v. 107 (B2), p. ETG 3-1-ETG 3-20, 2002. DOI: 10.1029/2000JB000044
79. WHIPPLE, K. X.; FORTE, A. M.; DIBIASE, R. A.; GASPARINI, N. M.; OUIMET, W. B. Timescales of landscape response to divide migration and drainage capture: Implications for the role of divide mobility in landscape evolution. **Journal Of Geophysical Research: Solid Earth**, v. 122, n. 1, p. 248-273, 2016. DOI: 10.1002/2016JF003973
80. WHITTAKER, A. C.; BOULTON, S. J. Tectonic and climatic controls on knickpoint retreat rates and landscape response times. **Geophysical Research Earth Surface**, v. 117, F02024, 2012. DOI: 10.1029/2011JF002157
81. WILLET, S. D.; BRANDON, M. T. On steady states in mountain belts. **Geology**, v. 30, n. 2, p. 175-178, 2002. DOI: 10.1130/0091-7613
82. WILLET, S.; MCCOY S. W.; PERRON, J. T.; GOREN, L.; CHEN, C.Y. Dynamic Reorganization of River Basins. **Science**, v. 343, n. 6175, 2014. DOI: 10.1126/science.1248765
83. WOBUS, C.; WHIPPLE, K.X.; KIRBY, E.; SNYDER, N.; JOHNSON, J.; SPYROPOLOU, K.; CROSBY, B.; SHEEHAN, D. Tectonics from topography: procedures, promise, and pitfalls. In: Willett, S.D.; Hovius, N.; Brandon, M.T.; Fisher, D.M. (Eds.). **Tectonics, Climate, and Landscape Evolution**. Geological Society of America Special Paper, v. 398, p. 55–74, 2006. DOI: 10.1130/2006.2398(04)
84. WOLPERT, J. A.; & FORTE, A. M. Response of transient rock uplift and base level knickpoints to erosional efficiency contrasts in bedrock streams. **Earth Surface Processes and Landforms**, v. 46, n. 10, p. 2092-2109, 2021. DOI: 10.1002/esp.5146
85. ZALÁN, P.V.; WOLFF, S.; CONCEIÇÃO, J.C.J.; MARQUES, A.; ASTOLFI, M.A.M.; VIEIRA, I.S.; APPI, V.T.; ZANOTTO, O.A. 1990. Bacia do Paraná. In: RAJA GABAGLIA, G.P.; MILANI, E.J. (Coords.). **Origem e evolução de bacias sedimentares.** PETROBRAS, p. 135-168, 1990.
86. ZOBACK, M. L. First- and Second-Order Patterns of Stress in the Lithosphere: The World Stress Map Project. **Journal of Geophysical Research**, v. 97, n. B8, p. 11703-11728, 1992. DOI: 10.1029/92JB00132